

## Exoplanets as New Sub-GeV Dark Matter Detectors

Rebecca K. Leane<sup>1,2,\*</sup> and Juri Smirnov<sup>3,4,†</sup><sup>1</sup>Center for Theoretical Physics, Massachusetts Institute of Technology, Cambridge, MA 02139, USA<sup>2</sup>SLAC National Accelerator Laboratory, Stanford University, Stanford, CA 94039, USA<sup>3</sup>Center for Cosmology and AstroParticle Physics (CCAPP),

The Ohio State University, Columbus, OH 43210, USA

<sup>4</sup>Department of Physics, The Ohio State University, Columbus, OH 43210, USA

(Dated: March 23, 2022)

We present exoplanets as new targets to discover Dark Matter (DM), with advantages due to their large expected abundance, low temperatures, and large sizes. Throughout the Milky Way, DM can scatter, become captured, deposit annihilation energy, and increase the heat flow within exoplanets. We estimate upcoming infrared telescope sensitivity to this scenario, finding actionable discovery or exclusion searches. We find that DM with masses above about an MeV can be probed with exoplanets, with DM-proton and DM-electron scattering cross sections down to about  $10^{-37} \text{cm}^2$ , stronger than existing limits by up to six orders of magnitude. Supporting evidence of a DM origin can be identified through DM-induced exoplanet heating correlated with Galactic position, and hence DM density. This also allows a potential tracer of DM overdensities. Our results provide new motivation to measure the temperature of the billions of brown dwarfs, rogue planets, and gas giants peppered throughout our Galaxy.

## I. INTRODUCTION

Are we alone in the Universe? This question has driven wide-reaching interest in discovering a planet like our own. Regardless of whether or not we ever find alien life, the scientific advances from finding and understanding other planets will be enormous. From a particle physics perspective, new celestial bodies provide a vast playground to discover new physics.

Astrophysical systems have already been broadly used to probe new physics, including investigating the effects of gravitationally captured Dark Matter (DM). This can occur if DM scatters with the system, loses energy, and becomes gravitationally bound. If there is sufficient gravitational force, deposited DM kinetic energy can noticeably increase the temperature of the system. Regardless of gravitational strength, DM annihilation can also induce heating. This has been investigated in the context of neutron stars and white dwarfs [1–39]. Alternatively, the DM-related heat flow in other moons and planets has been considered, including Earth [40–42], Uranus [43, 44], Neptune and Jupiter [44, 45], Mars [42], Earth’s Luna [46, 47], Jupiter’s Ganymede [48], as well as hot Jupiters [44].

We explore the potential to discover DM using *exoplanets* – planets outside our solar system. We will use the term “exoplanets” to refer to the broader class of all extra-solar planets (including rogue planets), as well as brown dwarfs, which exist at the planet-star boundary. There are many advantages of using exoplanets to search for DM over other celestial bodies. These include:

**A rapidly accelerating research program:** Until 1992, we didn’t even know if exoplanets existed. Al-

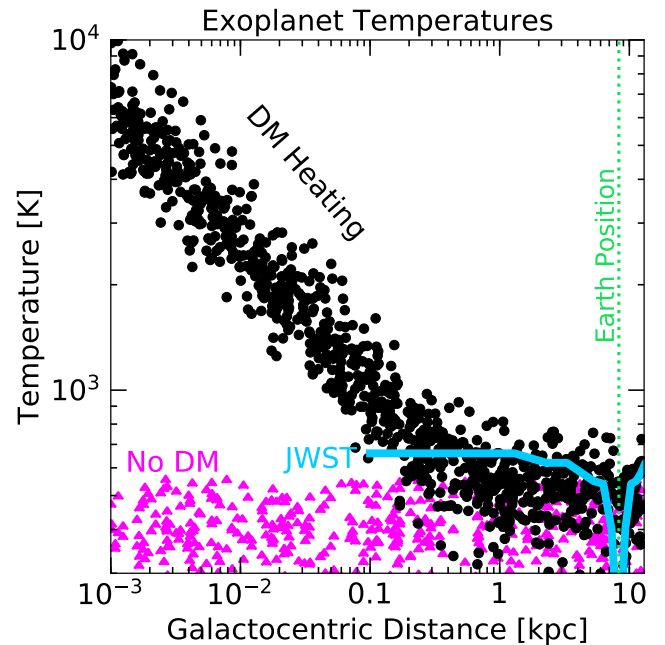


Figure 1. Mock temperature distribution of old example exoplanets with 20 – 50 Jupiter masses, as a function of distance from the center of our Galaxy. Black dots are DM-heated exoplanets, assuming a gNFW DM profile. The magenta triangles are the same set of planets, without DM heating. JWST is the estimated minimum telescope sensitivity (see text).

most all exoplanets we now know were only discovered in the last decade, with the majority found in the last five years [49]. The exoplanet program is clearly rapidly growing. Telescopes such as the James Webb Space Telescope (JWST), Transiting Exoplanets Survey Satellite (TESS), the Vera C. Rubin Observatory (Rubin, previously LSST), and the Nancy Grace Roman Space

\* Email: [rleane@slac.stanford.edu](mailto:rleane@slac.stanford.edu); ORCID: 0000-0002-1287-8780

† Email: [smirnov.9@osu.edu](mailto:smirnov.9@osu.edu); ORCID: 0000-0002-3082-0929

Telescope (Roman, previously WFIRST), and the Gaia Spacecraft have or will have targeted programs to discover as many exoplanets as possible. There are also many surveys such as the Optical Gravitational Lensing Experiment (OGLE), Two Micron All Sky Survey (2MASS), and the Wide-field Infrared Survey Explorer (WISE), which peer deep into our Galaxy. Further on the horizon, new telescopes are being planned or considered such as the Thirty Meter Telescope (TMT), the Extremely Large Telescope (ELT), Gaia Near Infra-Red (GaiaNIR), the Large Ultraviolet Optical Infrared Surveyor (LUVOIR), the Habitable Exoplanet Imaging Mission (HabEx), and the Origins Space Telescope (OST). These current and potentially upcoming telescopes can also observe exoplanets in new ways alongside other experiments, revealing even higher quality and more precise data. This provides ample motivation to consider new ways this exploding research area can be used to probe new physics.

**Enormous number of expected exoplanets:** It is estimated that there is at least one planet per star in our Galaxy, and about one cold planet per star [50]. This means that there should be about 300 billion exoplanets awaiting discovery. While of course these won't all be immediately found, even a small percentage of this number leads to an enormous statistical advantage for understanding potential signals. This makes exoplanets potentially more decisive than planets in our own solar system. It also allows ample room for growth with new discoveries and possible surprises in observations. To date, there are 4,284 confirmed exoplanets, and an additional 5,515 candidates are currently under investigation [49].

**Presence in non-local DM densities:** Exoplanets also abundantly exist in parts of the Milky Way where the local DM density is much larger, such as towards the Galactic Center (GC). This would provide a larger DM heating signal than a planet in our local DM density. The DM heating signal will then be correlated with the DM density, providing an additional handle on the DM distribution in our Galaxy. Provided sufficient sensitivity, it would also then be possible to confirm areas of DM overdensity, where the local density departs from expectations from DM density profile models.

**Much larger surface area than neutron stars:** The other key proposed search using upcoming infrared telescopes on DM-heated astrophysical bodies is with old, cold neutron stars [25]. However, while neutron stars are much more dense, and allow for higher heating rates in part due to enhancements from kinetic heating, exoplanets and brown dwarfs are *much* larger than neutron stars. A typical neutron star has a radius of about 10 km, while exoplanets of interest to us have radii of about 50,000 – 200,000 km. This means that exoplanet temperatures can be measured much further into the GC, as the spectral flux scales with the squared ratio of the radius of the object to the distance away. Neutron stars therefore do not have the advantage of potentially providing a DM-density dependent heating signal, as cold neutron stars

in enhanced DM density locations are too small to see at such distances (though see e.g. Ref. [51]). Inversely, this also means that closer-by exoplanets can be imaged to much higher significance, and with less exposure time.

**Easier to find than neutron stars:** The infrared neutron star search requires that a sufficiently cold neutron star candidate at a distance  $\lesssim 100$  pc from Earth is found [25]. While pulsars have been found at distances of  $\sim 100$  pc [52], it is possible that a sufficiently cold and sufficiently close-by neutron star may not ever be found, or cannot be measured with sufficient exposure time. On the other hand, exoplanets outnumber neutron stars in our galaxy by at least about a factor of a thousand [53], and are already known to exist in close enough proximity for DM searches, as we will show in this work.

**Low temperatures:** Lastly, exoplanets can be very cold, as they do not undergo nuclear fusion, and can exist very far in large orbits from any host star to which they may be bound. They can even go *rogue*, floating free from any parent star. As the low temperatures allow for a clearer signal over background for DM heating, exoplanets are advantageous over fuel-burning stars. Furthermore, their low core temperatures in part prevent DM evaporation compared to evaporation in these stars, providing new sensitivity to MeV DM.

In this work, we exploit all these features to identify new searches for DM in exoplanets. We establish two different searches: one for distant exoplanets and one for local exoplanets.

Figure 1 demonstrates these searches. We show an example distribution of exoplanets with masses of about 20 – 50 Jupiters, with and without DM heating. Distant exoplanets can be used to map the Galactic DM density, given sufficient telescope sensitivity. This is seen by the uptick of many hot exoplanets, scaling with the DM density. As well as broadly searching for DM signals, local exoplanets can be used to test the hypothesis that DM contributes to internal heat of the gas giants in our own solar system, which are not well understood [44, 45]. In both cases, DM-heated exoplanets can be potentially measured when the infrared telescope JWST comes online. Both our suggested searches target new DM parameter space, probing both the DM-proton and DM-electron scattering cross sections to unprecedented sensitivities. While the distant exoplanet search is certainly more challenging, the local exoplanet study can be expected to yield short-term results.

We organize our paper as follows. We begin in Section II by briefly outlining expected properties of exoplanets, as well as explicitly identifying known exoplanets as candidates for our proposed searches, and future prospects for exoplanet candidate discovery. We then quantify DM heating in exoplanets in Section III. In Section IV, we estimate the sensitivity with upcoming infrared telescopes, and discuss both opportunities and challenges for new DM-exoplanet searches. We then detail the reach these searches have on the DM parameter

space in Section V, determining the DM-proton and DM-electron scattering sensitivities across DM masses. We summarize and present our conclusions in Section VI.

## II. OVERVIEW OF EXOPLANETS

### A. Abundance and Properties

It is expected that on average, all stars have at least one planet [50]. Given we know there are about 300 billion stars in our Galaxy, this amounts to about 300 billion or more exoplanets in the Milky Way. Of these, there is a smorgasbord of exoplanet types, with diverse properties and sizes, which we briefly outline below.

#### 1. Earth-like Planets

The most popular exoplanet type for finding aliens are, of course, Earth-like planets. Earth-like planets have rocky interiors, and relatively small masses and radii relative to all other exoplanets. They extend into the “Super-Earths” category, which usually have radii of about that of Earth, but have up to a factor 10 higher in mass. These are not ideal for our DM searches, as their radii are smaller than other exoplanets, leading to limitations in telescope sensitivity. Interestingly however, it has been pointed out that DM annihilation heating of Earth-like exoplanets can lead to liquid water, and therefore a habitable planet, when otherwise the planet would have been too cold [54].

#### 2. Jupiters

The next-largest category is the gas giants, also called “Jovian planets” or “Jupiters”. Jupiters have radii roughly comparable to that of Jupiter, and generally have masses about comparable to Jupiter, though they can have up to about 10 times higher masses, becoming “Super Jupiters” (any higher, and they begin to transition into brown dwarf classification). Jupiters are one ideal class of exoplanets for our searches: they have large radii, and due to their lower mass compared to the next class, their internal heat flow can be very low. The minimum temperature expectation for Jupiters with masses and radii comparable to Jupiter, after 1 Gyr, is about 160 K [55]. After 10 Gyr, Jupiters are about 80 K [55]. Note that large cold gas giant planets are expected to be common [50, 56].

#### 3. Brown Dwarfs

Larger again are brown dwarfs, which were only discovered in 1995. Brown dwarfs are what lurk in the gap between gas giant planets and the least massive stars, placing them with masses of about 14–75 Jupiters. They generally have about the same radius as Jupiter, making them *immensely dense*. This makes brown dwarfs an

ideal candidate for our searches; they are large *and* dense. However, for our scenarios of interest we do not want to solely consider very massive brown dwarfs; too massive and they take longer to cool. This leads to a large heat background that might obscure DM heating signals. The minimum temperature expectation for brown dwarfs with masses of about 14–75, after 1 Gyr, is about 200–2000 K respectively [55, 57, 58]. After 10 Gyr, they range from about 150–750 K respectively [55, 57, 58]. This means that while brown dwarfs of all masses can be relevant for our study, internal heat from the heavier dwarfs may overpower DM heating in some DM densities/locations, or would only be relevant for our study if their age approached 10 Gyr. It will therefore depend on the candidate in question, whether its individual heat background is acceptable or not. In any case, the abundance of cold brown dwarfs is expected to be very high [50, 59]. More broadly, about 20% of stars are expected to have Jupiter-sized to brown dwarf sized planets [50]. Interestingly, brown dwarfs can have very exotic atmospheres, with some experiencing *iron rain* [60, 61]. Talk about a stormy day!

Brown dwarfs have been previously considered alongside DM, although in the context of asymmetric DM, which does not feature an annihilation heating signal, but rather a departure from the expected stellar evolution curve [62]. This is a similar approach to studying DM effects on stars in larger DM densities, such as in for example Refs. [63–80]. However, these have different observables to those pointed out in this work.

#### 4. Lost in Space: Rogue Planets

Not all planets have a home. A class of planets called “rogue planets” or “free-floating planets” have been ejected from their planetary nursery, damned to aimlessly wander, alone, through dark and empty space. While all planet types listed above can be rogue planets, Jupiters and brown dwarfs are by far the most common rogues. This lonely class of exoplanets is ideal for our searches. This is because they are free from light and heat pollution from any host star, allowing them to be more easily resolved. Similarly, at closer distances to Earth, Jupiters on larger orbits can be easier to distinguish than those closely bound to their star, for the same reason.

While rogue planets are currently thought to be less common than bound planets, they can still be extremely plentiful. The OGLE survey estimates that there is up to about one rogue for every 4 stars – that amounts to up to about 100 billion rogues in the galaxy [81]. Even more recently, a simulation of planetary systems in the Orion Trapezium Cluster showed that about 15% of all planets ended up ejected from orbit around their parent star [82]. (Interestingly, about 0.1% ended up being later welcomed into a new family, captured by another distant parent star.) Extrapolating this system, it implies that there could be about 50 billion rogue planets in our Galaxy [82]. Alternatively, brown dwarfs can have never had a host

star – they can form in molecular clouds like stars, and simply be all alone from the very beginning.

## B. Candidates and Further Discovery Potential

### 1. Local Planets

Table I lists some known Jovian planets within 100 pc, which are potential candidates for the local exoplanet search. These are chosen as examples based on their proximity, radii, masses, and orbital sizes. JWST may be able to image these planets, and probe new DM parameter space. Note however that some may turn out to have too much atmospheric cloud cover, or may be heated or obscured for other reasons. Regardless, there are many more potential candidates, which can be found in Ref. [49].

In addition to known candidates, many current and future telescopes will study our local neighborhood to identify and measure more candidate planets for DM heating. In particular, Gaia is expected to find  $21,000 \pm 6,000$  long-period Jupiters and brown dwarfs within 500 pc, within 5 years of operating [83]. Within 10 years, it is estimated to find  $70,000 \pm 20,000$  new exoplanets of interest [83]. This will substantially increase candidates and statistics for this search.

### 2. Distant Planets

The furthest planets ever found are SWEEPS-4 and SWEEPS-11 [113], which are about 8.5 kpc away (further than the Earth-GC distance). However, these planets are close to their host star, so are expected to be very hot (and therefore not ideal for DM heating searches). Many other planets are already known to exist, over varying distances from the GC. However, many of these planets are bound to a star. While this is helpful for discovery techniques (i.e. more techniques are available to discover planets bound to a star), this is not helpful for our searches in the galactic bulge. This is because, even while they still may have very large orbits, at the very far distances into the GC that we want to measure, they can be outshone by their bound host star, making temperature measurements impossible. We therefore focus on rogue planets when examining potential DM signals at large distances.

While rogue planets are harder to find, some have already been found, and it is expected that many more can be found soon. Such searches require use of gravitational microlensing, which can be aided especially with simultaneous use of telescopes, allowing for more decisive confirmation of planetary status. For example, this has been achieved with Roman and Euclid [114].

OGLE has been operating since 1992, focusing on searches in the stellar bulge. It has already identified many distant exoplanets and exoplanet candidates. For

rogue planet candidates, this includes e.g. OGLE-2019-BLG-0551 [115], and a brown dwarf candidate OGLE-2015-BLG-1268, with 50 Jupiter masses and at  $5.9 \pm 1.0$  kpc [116]. Spitzer has observed a candidate together with OGLE, called OGLE-2017-BLG-0896, which is potentially a brown dwarf about 4 kpc towards the bulge [117]. OGLE is still very active, and will be important for identifying more candidates in the future.

In the near future, Roman is expected to find about 2200 new cold planets towards the galactic bulge (2000 of which have mass greater than Earth) [118], and hundreds of free-floating planets [119]. Our exoplanet searches benefit from large statistical samples, which Roman could provide. It aims to perform a deep near-infrared survey of the Galactic sky, and upon identifying candidates, can inform infrared telescopes such as JWST where to measure the temperature of the candidate planet. Alternatively, if a K-filter is added to Roman (allowing it to see further into the infrared) it itself may be able to measure the temperature of colder exoplanets [120].

## C. Temperature and Density Profiles

To study Jupiters, we use the profile models for our Jupiter, as per Ref. [121]. This features a core temperature of  $T_c = 1.5 \times 10^4$  K, an average density of  $\rho_{\text{jup}} = 1.3 \text{ g/cm}^3$ , and a radius of  $R_{\text{jup}} = 6.99 \times 10^7$  m. We set our benchmark Jupiters to all have the same radius as Jupiter. We also check if results vary with two different Jupiter density profile hypotheses, one with a core and the other without [121]. For our parameters of interest, there is no noticeable effect.

To study brown dwarfs, we use the analytical model from Ref. [122]. The brown dwarf radius, core density and core temperature can be expressed as a function of mass and electron degeneracy,

$$R = 2.81 \times 10^9 \left( \frac{M_\odot}{M} \right) \mu_e^{-5/3} (1 + \gamma + \alpha\psi) \text{ cm}, \quad (1)$$

$$\rho_c = 1.28 \times 10^5 \left( \frac{M_\odot}{M} \right)^2 \frac{\mu_e^5}{(1 + \gamma + \alpha\psi)^3} \text{ g/cm}^3, \quad (2)$$

$$T_c = 7.86 \times 10^8 \left( \frac{M_\odot}{M} \right)^{4/3} \frac{\mu_e^{8/3} \psi}{(1 + \gamma + \alpha\psi)^2} \text{ K}. \quad (3)$$

Here,  $\mu_e$  is the number of electrons per baryon,  $\psi$  the electron degeneracy parameter and  $\gamma$  is a higher-order correction factor (see Ref. [122] for a detailed discussion). There is a particular electron degeneracy at which the core temperature reaches its maximum, and drops to smaller values if the degeneracy is further increased. Once the brown dwarf passes this point in the cooling process, its core temperature decreases significantly, while its density grows. The relatively low core temperatures and high densities make old brown dwarfs efficient accumulators for light DM. For our benchmark, the brown dwarf (BD) radius is taken to be  $R_{\text{BD}} = R_{\text{jup}}$ , and



Planet	Radius ( $R_{\text{jup}}$ )	Mass ( $M_{\text{jup}}$ )	Distance	Orbit	Temp (No DM)	Temp (with DM)	Ref
Epsilon Eridani b	1.21	1.55	3 pc	3.4 au	$\lesssim$ 200 K	$\lesssim$ 650 K	[84]
Epsilon Indi A b	1.17	3.25	3.7 pc	11.6 au	$\lesssim$ 200 K	$\lesssim$ 650 K	[85]
Gliese 832 b	1.25	0.68	4.9 pc	3.6 au	$\lesssim$ 200 K	$\lesssim$ 650 K	[86]
Gliese 849 b	1.23	1.0	8.8 pc	2.4 au	$\lesssim$ 200 K	$\lesssim$ 650 K	[87]
Thestias	1.19	2.3	10 pc	1.6 au	$\lesssim$ 200 K	$\lesssim$ 650 K	[88]
Lipperhey	1.16	3.9	12.5 pc	5.5 au	$\lesssim$ 200 K	$\lesssim$ 650 K	[89]
HD 147513 b	1.22	1.21	12.8 pc	1.3 au	$\lesssim$ 200 K	$\lesssim$ 650 K	[90]
Gamma Cephei b	1.2	1.85	13.5 pc	2.0 au	$\lesssim$ 200 K	$\lesssim$ 650 K	[91]
Majriti	1.16	4.1	13.5 pc	2.5 au	$\sim$ 218 K	$\lesssim$ 650 K	[92]
47 Ursae Majoris d	1.2	1.64	14 pc	11.6 au	$\lesssim$ 200 K	$\lesssim$ 650 K	[93]
Taphao Thong	1.2	2.5	14 pc	2.1 au	$\lesssim$ 200 K	$\lesssim$ 650 K	[93]
Gliese 777 b	1.21	1.54	15.9 pc	4.0 au	$\lesssim$ 200 K	$\lesssim$ 650 K	[94]
Gliese 317 c	1.21	1.54	15.0 pc	25.0 au	$\lesssim$ 200 K	$\lesssim$ 650 K	[95]
q <sup>1</sup> Eridani b	1.23	0.94	17.5 pc	2.0 au	$\lesssim$ 200 K	$\lesssim$ 650 K	[87]
HD 87883 b	1.21	1.54	18.4 pc	3.6 au	$\lesssim$ 200 K	$\lesssim$ 650 K	[96]
$\nu^2$ Canis Majoris c	1.24	0.87	19.9 pc	2.2 au	$\lesssim$ 200 K	$\lesssim$ 650 K	[97]
Psi <sup>1</sup> Draconis B b	1.21	1.53	22.0 pc	4.4 au	$\lesssim$ 200 K	$\lesssim$ 650 K	[98]
HD 70642 b	1.19	1.99	29.4 pc	3.3 au	$\lesssim$ 200 K	$\lesssim$ 650 K	[99]
HD 29021 b	1.2	2.4	31 pc	2.3 au	$\lesssim$ 200 K	$\lesssim$ 650 K	[100]
HD 117207 b	1.2	1.9	32.5 pc	4.1 au	$\lesssim$ 200 K	$\lesssim$ 650 K	[101]
Xolotlan	1.2	0.9	34.0 pc	1.7 au	$\lesssim$ 200 K	$\lesssim$ 650 K	[102]
HAT-P-11 c	1.2	1.6	38.0 pc	4.1 au	$\lesssim$ 200 K	$\lesssim$ 650 K	[103]
HD 187123 c	1.2	2.0	46.0 pc	4.9 au	$\lesssim$ 200 K	$\lesssim$ 650 K	[104]
HD 50499 b	1.2	1.6	46.3 pc	3.8 au	$\lesssim$ 200 K	$\lesssim$ 650 K	[101]
Pirx	1.2	1.1	49.4 pc	0.8 au	$\sim$ 200 K	$\lesssim$ 650 K	[105]
HD 27631 b	1.2	1.5	50.3 pc	3.2 au	$\lesssim$ 200 K	$\lesssim$ 650 K	[106]
HD 6718 b	1.2	1.7	51.5 pc	3.6 au	$\lesssim$ 200 K	$\lesssim$ 650 K	[107]
HD 72659 b	1.2	3.9	52.1 pc	4.8 au	$\lesssim$ 200 K	$\lesssim$ 650 K	[108]
HD 4732 c	1.2	2.4	54.9 pc	4.6 au	$\lesssim$ 200 K	$\lesssim$ 650 K	[109]
HD 290327 b	1.2	2.4	56.4 pc	3.4 au	$\lesssim$ 200 K	$\lesssim$ 650 K	[107]
HD 154857 c	1.2	2.6	63.5 pc	5.4 au	$\lesssim$ 200 K	$\lesssim$ 650 K	[110]
Drukyul	1.2	1.6	83.4 pc	2.9 au	$\lesssim$ 200 K	$\lesssim$ 650 K	[111]
Kepler-539 c	1.18	2.4	92 pc	2.7 au	$\lesssim$ 200 K	$\lesssim$ 650 K	[112]

Table I. List of some candidate Jupiters within 100 pc, to use in a near-Earth search. Distance is quoted as from the Earth. The predicted temperature ranges include generic estimates for emissivity and planetary mass. Masses, radii, orbits, and distances from Earth are estimates taken from the NASA exoplanet catalog [49].

the mass  $M_{\text{BD}} = 75 M_{\text{jup}} = 0.075 M_{\odot}$ . This results in an average density of  $\rho_{\text{BD}} = 103 \text{ g/cm}^3$ , a core density of  $\rho_c = 500 \text{ g/cm}^3$  and a core temperature  $T_c = 2 \times 10^5 \text{ K}$ . Note that in the analytic model, fusion heating is not included. Our calculations are therefore only relevant in the regime where there is no fusion, which is appropriate to obtain lower internal heat backgrounds.

### III. DARK HEAT FLOW IN EXOPLANETS

#### A. Dark Matter Densities

To calculate the DM-heating rate in exoplanets, we consider different DM profiles, which control the amount of DM available for heating at a given location in our Galaxy. We consider a Navarro-Frenk-White (NFW) profile, a generalized NFW (gNFW) profile, and a Burkert profile. The NFW profile is defined as a density as a function of galactic radius [123]

$$\rho_{\chi}(r) = \frac{\rho_0}{(r/r_s)^{\gamma}(1+(r/r_s))^{3-\gamma}} \quad (4)$$

where we take a scale radius of  $r_s = 8 \text{ kpc}$  [130] (larger choices of e.g.  $r_s = 20 \text{ kpc}$  do not significantly change the results). The standard NFW profile has  $\gamma = 1$ , while the generalized NFW profile is taken to have a steeper inner slope of  $\gamma = 1.5$  (this is equivalent to a Moore profile). This steeper value represents a more contracted profile, which can arise due to adiabatic contraction. Note that hydrodynamical simulations can sometimes produce even larger values of the inner slope [124].

Lastly, we also consider a cored profile, called the Burkert profile [125],

$$\rho_{\chi}(r) = \frac{\rho_0}{(1+r/r_{\text{sb}})(1+(r/r_{\text{sb}})^2)}. \quad (5)$$

For this profile, we will take a smaller core radius, such that  $r_{\text{sb}} = 0.5 \text{ kpc}$ , to demonstrate reasonable variations in the profiles (as per Ref. [126]). Note however that in principle the core radius could be larger for this profile, making the DM density smaller towards the GC.

For all these profiles, we normalize to the local DM density value of  $0.42 \text{ GeV/cm}^3$  [127]. While we only consider variations of these profiles in our calculations, it is expected that overdensities – localized regions of increased DM – likely exist, and would be potentially detectable as hot exoplanets would deviate from the expectations of the profiles above, which we will also briefly investigate.

#### B. Heating Rates

##### 1. Total Heat Flow

The total heat flow of the exoplanet  $\Gamma_{\text{heat}}^{\text{tot}}$  can be determined by combining potential heat power sources, including internal heat  $\Gamma_{\text{heat}}^{\text{int}}$ , external heat  $\Gamma_{\text{heat}}^{\text{ext}}$ , and DM

heat  $\Gamma_{\text{heat}}^{\text{DM}}$ :

$$\Gamma_{\text{heat}}^{\text{tot}} = \Gamma_{\text{heat}}^{\text{ext}} + \Gamma_{\text{heat}}^{\text{int}} + \Gamma_{\text{heat}}^{\text{DM}} = 4\pi R^2 \sigma_{\text{SB}} T^4 \epsilon, \quad (6)$$

where  $R$  is the exoplanet radius,  $T$  is the exoplanet temperature (without other heat sources),  $\sigma_{\text{SB}}$  is the Stefan-Boltzmann constant, and  $\epsilon$  is for emissivity of the planet, and external heating is taken to be negligible for wide-orbit or free-floating planets. Emissivity captures how effective the planet is at radiating heat, and ranges from 0 to 1. A more dense atmosphere often leads to a lower emissivity value; this can be caused, for example, by greenhouse effects on the planet. The emissivity can in principle be determined from spectroscopy studies. For reference, Earth has an emissivity value of 0.6, our Jupiter is about 0.9, and Venus is about 0.004 [54]. Typically, larger or more dense planets have lower emissivities, though this can largely vary depending on the candidate planet. The internal heat flow is a conserved quantity, and so decreasing emissivity below one will lead to higher planetary temperatures, balancing Eq. 6. We now consider the individual heating components.

##### 2. Internal Heat Flow (Without DM)

We compute the internal heat flow for our range of benchmark brown dwarfs and Jupiters without DM. As the minimum temperature for heavy brown dwarfs (with  $75 M_{\text{jup}}$ ) and benchmark Jupiters (with  $M_{\text{jup}}$ ) after about 10 Gyr is about 750 K and 80 K respectively, we can determine the internal heat flow required to produce these temperatures,

$$\Gamma_{\text{heat}}^{\text{int}} = 4\pi R^2 \sigma_{\text{SB}} T^4 \epsilon, \quad (7)$$

we get internal heat flow values of about  $1.1 \times 10^9 \text{ TW}$  and  $1.4 \times 10^5 \text{ TW}$  for brown dwarfs and Jupiters, respectively. This assumes that no DM heating is present, and a planet is sufficiently far away from any external heating source such as a host star. It will serve as our non-DM baseline for comparing with a potential DM signal.

##### 3. Dark Matter Heat Flow

We now consider contributions from DM heating. This can proceed as DM scatters on exoplanet protons, and becomes captured. The captured DM then can annihilate, producing heat that can be absorbed by the exoplanet. We assume that the DM scattering and annihilation processes are in equilibrium, which is expected for such large rates (see Sec. V C). Unlike the internal heat flow from SM processes, the DM heat flow depends on how many external DM particles are captured from the incoming DM flux reservoir. The amount of captured DM will depend on the DM masses and cross sections (see Sec. V A).

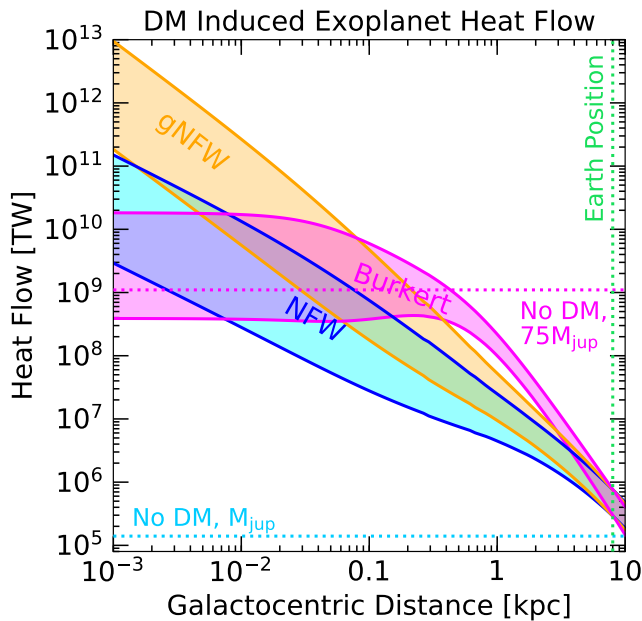


Figure 2. Exoplanet heat power as a function of distance from the center of our Galaxy. Solid lines shown are the DM-heat power of exoplanets with radius  $R_{\text{jup}}$ , with a range of masses from  $M_{\text{jup}}$  (lower line) up to  $75 M_{\text{jup}}$  (upper line). The shaded region corresponds to DM-heat power for intermediate exoplanet masses. The dotted lines show the range of heat power for the heaviest dwarfs (with  $75 M_{\text{jup}}$ ) down to the lighter benchmark Jupiters (with  $M_{\text{jup}}$ ) in the absence of DM or external heat.

The maximal capture rate (also known as geometric capture rate) of DM is given by [128]

$$C_{\text{max}} = \pi R^2 n_{\chi}(r) v_0 \left( 1 + \frac{3}{2} \frac{v_{\text{esc}}^2}{v_d(r)^2} \right) \xi(v_p, v_d(r)), \quad (8)$$

where  $n_{\chi}(r)$  is the DM number density at distance  $r$  from the GC, the average speed in the DM rest frame  $v_0$  is related to the velocity dispersion  $v_d(r)$  as  $v_0 = \sqrt{8/(3\pi)} v_d(r)$  at distance  $r$  from the GC, and  $R$  is the exoplanet radius. The factor  $1 + 3 v_{\text{esc}}^2 / 2 v_d^2$  is the result of gravitational focusing, with  $v_{\text{esc}}^2 = 2G_N M / R$  being the escape velocity,  $M$  the exoplanet mass, and  $G_N$  the gravitational constant. The motion of the planet with velocity  $v_p$  with respect to the DM halo is taken into account by  $\xi(v_p, v_d(r))$ . In the scenarios we are interested in, the DM velocity, the planetary velocity and the escape velocities are of similar order and the function  $\xi(v_d(r), v_p) \sim 1$ . The circular velocities  $v_c(r)$  in the galaxy are related to the DM velocity dispersion by  $v_d(r) = \sqrt{3/2} v_c(r)$ . We extract the circular velocities at different radii in the Milky Way by combining the data for the gas, bulge, and disk components, as well as the analytic expressions for DM contributions to the total velocity from Ref. [130].

The heat power produced by DM is given by the product of the DM mass  $m_{\chi}$ , the fraction of the captured DM particles that have passed through the object  $f$ , and the

maximal capture rate, such that

$$\Gamma_{\text{heat}}^{\text{DM}} = m_{\chi} f C_{\text{max}}. \quad (9)$$

Using  $n_{\chi}(r) = \rho_{\chi}(r)/m_{\chi}$ , approximating  $\xi(v_d(r), v_p) \sim 1$ , and combining with Eq. 8, the DM heat power can be written as

$$\Gamma_{\text{heat}}^{\text{DM}} = f \pi R^2 \rho_{\chi}(r) v_0 \left( 1 + \frac{3}{2} \frac{v_{\text{esc}}^2}{v_d(r)^2} \right). \quad (10)$$

We see that the DM heat flow is independent of DM mass. This is because the heat flux scales as  $1/m_{\chi}$ , and each DM particle releases an amount of energy equal to  $m_{\chi}$  once annihilating.

Another type of potential DM heating is kinetic DM heating. This arises when astrophysical systems have steep gravitational wells, causing DM to be accelerated to speeds near that of light. However, even for dense brown dwarfs, the escape velocity is only about  $0.001c$ , rendering any DM kinetic heating negligible.

Figure 2 shows the calculated heat flow from DM or internal heat, as a function of galactic radius. DM-heating arising due to several different DM profiles is shown, for NFW, gNFW, and Burkert profiles. The lower line shows the heat power prediction for exoplanets of mass  $M_{\text{jup}}$ , while the upper line shows DM-heating for heavy brown dwarfs ( $75 M_{\text{jup}}$ ). All planetary radii  $R$  are taken to be  $R_{\text{jup}}$ , which is the radius for all old brown dwarfs or Jupiters. Here, it is assumed that all of the DM passing through the planet is captured ( $f = 1$ ). Any sub-maximal DM capture would lead to a heat power simply rescaled linearly with  $f$ . The shaded region for a given DM profile shows the intermediate temperatures for any Super Jupiter or lighter brown dwarf. The dotted lines show the internal heat for the two benchmark cases ( $M_{\text{jup}}$  vs  $75 M_{\text{jup}}$ ) without DM heating, after 10 Gyr. Intermediate exoplanet masses without DM heating will fall between these lines. We see that for Jupiters (lower solid line), the DM heat will outperform the internal heat at all radii, making them ideal candidates for all searches. Brown dwarfs, on the other hand, being more dense, have higher internal heat, and DM heating will only clearly outperform their internal heat for some DM densities and radii.

The shape of the curves in Fig. 2 as a function of galactic radius is due to an interplay of the DM density profile, the DM velocity profile, and the effective capture radius of the exoplanet, which varies as a function of the DM velocity. That is, while the DM density increases closer to the GC, the DM velocity substantially decreases, while the effect of gravitational focusing at low velocities boosts the heating rate.

#### IV. SEARCHES AND INFRARED TELESCOPE SENSITIVITY

We now discuss two different searches: a local search, and a distant search. Exoplanets may first be identi-

fied by e.g. Doppler spectroscopy (radial-velocity) methods, transit photometry, direct imaging, or gravitational lensing. Once their location is found, infrared telescopes such as JWST may be able to measure their temperature. This temperature will depend on the DM density to different amounts, which provides a DM-correlated signal for the two searches we detail below.

### A. Fluxes and JWST Exoplanet Sensitivity

The general sensitivity of JWST to exoplanet heating can be found by considering the spectral flux density,

$$f_\nu = \pi B(\nu, T) \times \frac{4\pi R^2}{4\pi d^2}, \quad (11)$$

where  $d$  is the distance from the telescope to the exoplanet,  $R$  is the radius of the exoplanet, and

$$B(\nu, T) = \frac{2\nu^3 \epsilon}{\exp\left(\frac{2\pi\nu}{k_b T}\right) - 1}, \quad (12)$$

where  $\nu$  is the wavelength,  $T$  is the temperature,  $k_b$  is the Boltzmann constant, and  $\epsilon$  is the atmospheric emissivity. While  $\epsilon = 1$  provides the usual blackbody spectral flux density, deviations from a blackbody occur when the emissivity value is smaller than one; see Appendix A for more details on the impact this has on telescope sensitivity. The spectral flux density for a given exoplanet can be compared to a variety of instruments and filters as part of JWST, to determine the optimal sensitivities. Note that to be conservative, we will not add the DM-heated spectrum on top of the existing spectrum of dwarfs (which could be relevant at low temperatures), and rather will assume that the DM-heated temperature is the peak setting the sensitivity limit.

Figure 3 shows the expected exoplanet temperature as a function of distance from the center of the Galaxy, for DM-heating arising due to several different DM profiles: NFW, gNFW and a Burkert profile. We distinguish between Jovian exoplanets with masses between  $1 - 14 M_{\text{jup}}$  and brown dwarfs with masses in the range of  $14 - 75 M_{\text{jup}}$ . The brown dwarfs are again sub-divided into three mass ranges. All exoplanets shown have a radius of  $R_{\text{jup}}$ , as all these exoplanets are expected to converge to this radius after 10 Gy. Each panel has emissivity equal to one (i.e. a blackbody spectrum is assumed), which is the most conservative case (see Appendix A for details on how other emissivity choices can further increase the temperature due to DM). The shaded region for a given DM profile represents the range of heating possibilities for the indicated mass range, with the heaviest exoplanets lying at the upper boundary and the lightest exoplanets lying at the lower boundary. The shape of the curves as a function of galactic radius is due to an interplay of the DM density profile, the DM velocity profile, and the effective capture radius of the exoplanet, which varies as a function of the DM velocity. That is, while

the DM density increases closer to the GC, the DM velocity substantially decreases. Furthermore, the effect of gravitational focusing at low velocities boosts the heating rate, especially for larger planetary masses.

The dotted lines in Fig. 3 are the temperatures for the same ranges of exoplanets, without DM heating. Exoplanets without DM heating that have masses between the masses labeled, would have temperatures between these dotted lines. As heavier exoplanets have higher levels of internal heating, the total heat at higher masses approaches the internal heat value when there is not much DM heating available (e.g. at the local position). The top-left panel shows that, for Jupiters, for the lighter masses (lower line) the DM heating can outperform the internal heat at all locations, as the internal heat is so low.

We show in Fig. 3 the optimal JWST sensitivity, which is found using Eq. 11 above, with the benchmark dwarf/Jupiter radius of  $R_{\text{jup}}$ . This is calculated using different JWST instruments: the NEAR-INFRARED IMAGER AND SLITLESS SPECTROGRAPH (NIRISS) in IMAGING mode for temperatures above about 500 K, and the MID-INFRARED INSTRUMENT (MIRI) in IMAGING or MEDIUM-RESOLUTION SPECTROSCOPY mode for temperatures from about 100 – 500 K. As different JWST instrument filters are optimized for different flux densities/temperatures, we use several different filters while scanning over the minimal temperature measurable, to obtain the optimal sensitivity. In Fig. 3, the dashed line is for JWST to obtain about  $10^5$  seconds of exposure to achieve a signal-to-noise ratio (SNR) of 2. 10 SNR can be achieved at about  $10^6$  seconds of exposure at the most of the temperatures shown (though depending on the filter it can approach a factor of few times  $10^6$  for 10 SNR). Note however that these exposure times are for the minimum temperatures on the dashed line; higher temperatures generally require less exposure time. Exposure times of up to around  $10^6$  seconds are achievable with deep field survey; a survey of the GC is very well-motivated for numerous reasons even separate to our work. Significantly less time is required to achieve 10 SNR in the local region; more detailed JWST sensitivity estimates are discussed in the context of the searches below.

From Fig. 3, it is clear that different types of exoplanets have different regimes where they are most useful as a DM heating target. The lower mass Jupiters are ideal for local searches, as they outperform their internal heat at the Earth position. For higher mass brown dwarfs, their internal heat is too high to reveal a DM heating signal at the Earth position. However, their larger masses are advantageous at larger distances and/or in more DM dense areas. This is because gravitational focusing allows them to collect more DM. This allows us to identify two different searches: one for DM in local Jupiters, and another for all exoplanets (but especially those with higher-masses) at larger distances, in DM dense regions.



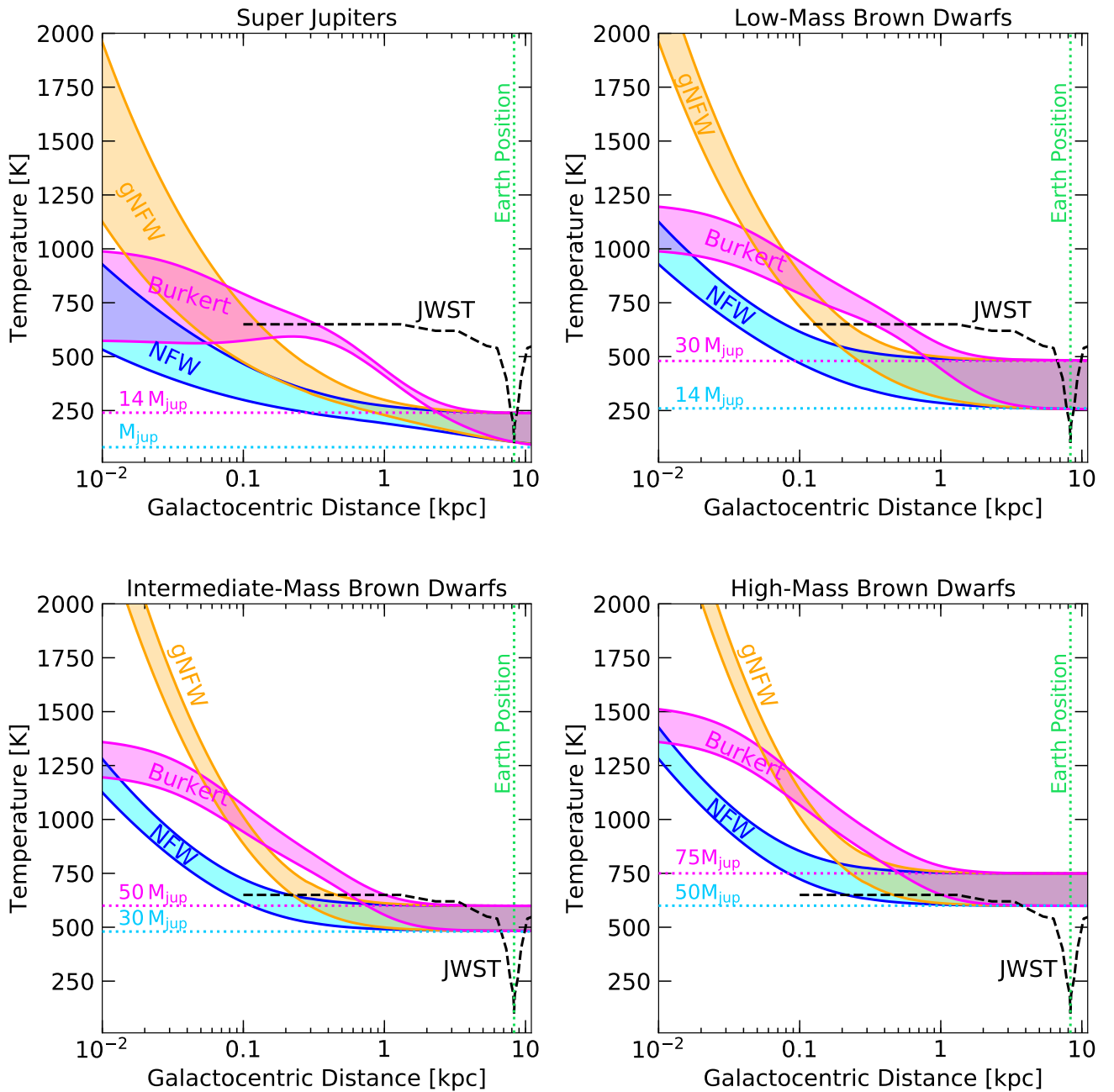


Figure 3. Exoplanet temperatures as a function of distance from the center of our Galaxy, with variations due to DM for labeled density profiles (assuming no DM overdensities). Each panel represents our classification of different exoplanet types: Super Jupiters ( $M_{\text{jup}} - 14 M_{\text{jup}}$ ), low-mass brown dwarfs ( $14 M_{\text{jup}} - 30 M_{\text{jup}}$ ), intermediate-mass brown dwarfs ( $30 M_{\text{jup}} - 50 M_{\text{jup}}$ ) and high-mass brown dwarfs ( $50 M_{\text{jup}} - 75 M_{\text{jup}}$ ). Any exoplanet within the indicated mass range will have temperatures between these lines in the shaded region, with the heaviest exoplanets at the upper boundary and the lightest exoplanets at the lower boundary. The dotted lines show the range of minimum temperatures for a 10 Giga-year-old exoplanet without DM; similarly any exoplanet within the indicated mass interval without DM heating has temperatures between these dotted lines. Black dashed line is the optimal minimum JWST sensitivity; anything above the line can potentially be probed (see text).

### B. First Search: DM in Local Jupiters

Our first search is for local Jupiters. As the Jupiters can have lower internal temperatures compared to a brown dwarf at the same age, they are more likely to

be found at lower temperatures. This means that closer to Earth, where the DM heating is lower, they are ideal search candidates to ensure the DM heating outperforms the background internal heating. This is clear from examining the JWST dip in Fig. 3 at the Terra position,

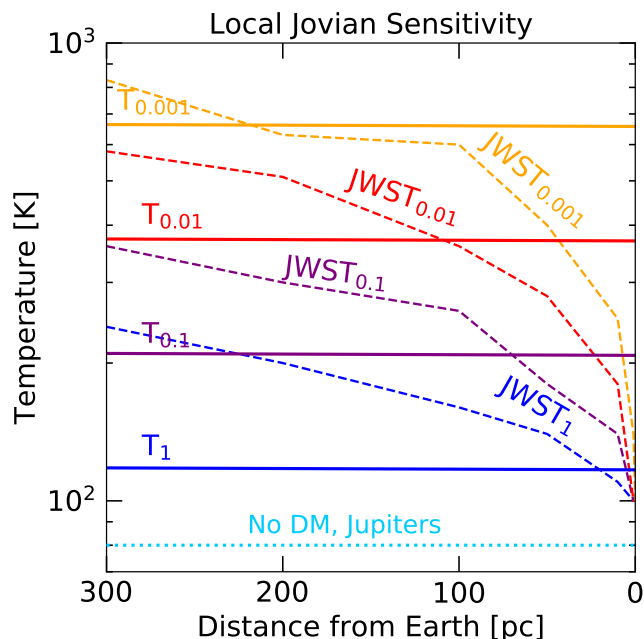


Figure 4. Expected temperatures of local Jovian planets with masses of  $M_{\text{jup}}$ . Increased temperatures due to DM-heating and varying emissivity values  $\epsilon$  are shown as  $T_\epsilon$  (solid lines), where distances shown are towards the GC. Corresponding best JWST sensitivities for each emissivity value are shown as  $\text{JWST}_\epsilon$ , as a function of the target-earth distance (dashed lines). We also show the temperature of an  $\epsilon = 1$  Jupiter without DM heating (dotted).

and comparing the temperatures from internal heat alone from the types of exoplanets.

Nearby Jupiters, especially if DM heated, are within reach of direct imaging with JWST. This is an interesting possibility, as the gas giants of our own solar system are not well understood, and it could corroborate any potential DM contributions to their internal heat. Alternatively, measurement of a few sufficiently cold exo-Jupiters would exclude this hypothesis, and allow for a DM scattering constraint to be set (see Sec. V).

Figure 4 shows the expected exoplanet temperature as a function of distance from the center of the Galaxy, for Jupiters with different emissivities. We also show the optimal minimal JWST temperature sensitivity, for varying emissivity values. The JWST lines are found using the MIRI: IMAGING instrument, with 2 SNR in  $10^5$  seconds. Anything above this line requires comparable or shorter exposure times, for the given emissivity. For example, for a Jupiter within 10 pc, only about 50 seconds of exposure time is needed in the maximally DM-heated scenario (650 K, emissivity 0.001) to achieve 10 SNR (using NIRISS in IMAGING mode). At 100 pc, 10 SNR can be achieved in about  $10^5$  seconds. The weakened JWST sensitivities for decreasing emissivity values are due to the spectral flux having a lower normalization proportional to emissivity; see Appendix A for more details. The dotted line

shows the temperature of a 10 Gyr Jupiter with no DM heating, for emissivity equal to one. The non-DM temperature for smaller emissivities may scale proportionally as  $T/\epsilon^{1/4}$ , however, the emissivity value may be affected by feedback effects in the cooling process. Note that even cold (non-DM heated) Jovian planets have been found to be possible to detect, in a more detailed JWST potential sensitivity analysis [131].

While the brown dwarf internal heating overpowers DM heating given local DM density, making them non-optimal targets for local searches, their high internal heat can be advantageous for another search strategy. The local relative abundance of dwarfs compared to other stellar populations, and the age/temperature distribution of the dwarfs can be determined, and can be potentially used to extrapolate to expected temperature/abundances towards the GC. This will be relevant for the distant search we now discuss below, as this would generate an apparent overabundance of younger brown dwarfs.

### C. Second Search: DM Density Correlated Hot Distant Exoplanets

Our second, more ambitious search, is for distant exoplanets. As shown in Fig. 3, at further radii, exoplanets increasingly are heated by DM, proportionally with the increase in DM density. This means that exoplanets can in principle to be used to trace the DM density in our Galaxy. This also means that, given a particularly large statistical sample, DM overdensities could also be revealed by too many hot exoplanets in a given region. Compared to the local search above, the distant search is relevant for both Jupiters and brown dwarfs, as old Jupiters and brown dwarfs can both be DM-heated potentially well above their expected internal heat. As Fig. 3 shows, the smoking-gun signal of this search is a rising exoplanet temperature towards the GC, consistent with DM profile expectations.

To demonstrate sensitivity to an example DM-heated large-distance exoplanet, we consider an exoplanet with radius  $R_{\text{jup}}$  at a distance from Earth of 8.2 kpc, which sits off the plane by 0.1 kpc. Given its location, for a mass of about  $14 M_{\text{jup}}$ , a DM-heated temperature of roughly 800 K would be obtained (assuming the gNFW profile), leading to a wavelength of  $\nu^{-1} = 3.6$  microns, and a flux density (using Eq. 11) of  $f_\nu = 1.4$  nJy. This can be in principle measured by JWST using the NIRISS: IMAGING mode, and the F356W filter, at 4 SNR with about  $10^5$  seconds of exposure. With about  $10^6$  seconds of exposure and the same filter, this can be detected at 10 SNR. In comparison, without DM heating, this exoplanet would have a temperature of around 220 K if sufficiently old and isolated, and so such a large increase in temperature would present as evidence for DM heating.

Figure 5 demonstrates more generally how DM densities may be identified or excluded with exoplanets. For the Jupiter benchmark shown, no planets should be found

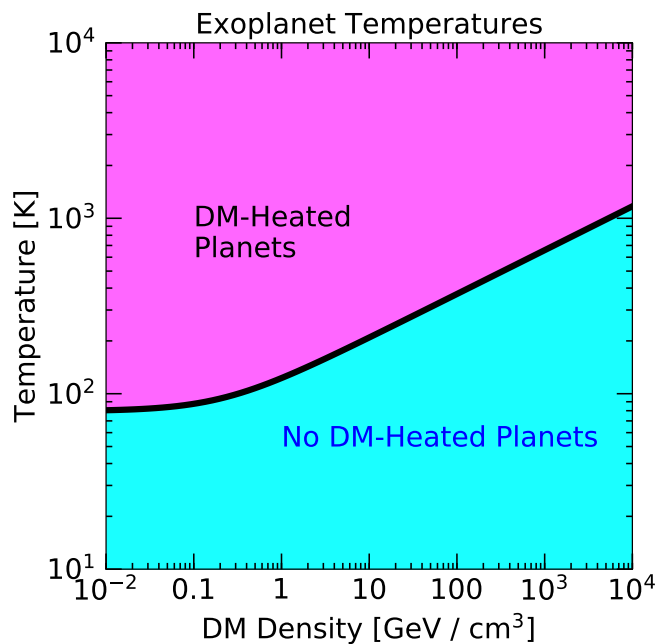


Figure 5. Minimum DM-heated exoplanet temperature as a function of DM density, for a Jupiter-like planet with mass  $M_{\text{jup}}$  and radius  $R_{\text{jup}}$ . A positive signal would lead to all planets being found in the “DM-Heated Planets” region, and none in the “No DM-Heated Planets” region.

in the DM densities given with the low temperatures as shown. On the other hand, all planets measured would be found in the DM-heating region. Any measurement contrary to this prediction would lead to an exclusion. In this figure, the DM velocity is set to 230 km/s – the local DM velocity around a given candidate would need to be scaled in, along with gravitational focusing if the exoplanet is present in a low-DM velocity environment. The emissivity of the exoplanets in this plot is set to 1; this is a conservative choice, as lower emissivity values simply lead to higher DM-heating values. Note that overdensities of DM are expected from  $N$ -body simulations, such as VIA LACTEA [132, 133], GALHO [134], and AQUARIUS [135]. It has been shown that the dense cores of many of the merging haloes that made our Milky Way survive as DM subhaloes, leading to e.g. DM streams or clumping. These overdensities or subhaloes can potentially be independently identified by gravitational microlensing (see e.g. Ref. [136]).

#### D. Challenges and Opportunities

We have presented optimal estimates for JWST sensitivity, which take into account some effects that degrade the sensitivity. We now briefly discuss assumptions and estimates of the impact of these effects, and discuss directions to overcome some of these challenges.

#### 1. Planet-Star Separation

Bound planets, at large distances, will invariably be too small to resolve with JWST, and will be outshone by their parent star. As such, we only consider free-floating planets for the distant search. However, for the local search, it is possible with JWST to observe bound planets, as they can be close enough to be resolved. Regardless, planets on wider orbits are still preferable candidates even for the local search, as they are easier to disentangle from their star. An additional bonus for targeting planets on wider orbits, is that they are likely to have lower temperatures (as they receive less heat from their star).

#### 2. Planet Emissivities

In Fig. 4, we display a range of emissivities. These correspond to how efficiently the planet radiates heat; a lower emissivity will lead to more heat becoming trapped. While Fig. 4 showed fixed emissivities for each plot, in a true search, a given planet can have different emissivity values at different temperatures. To know where the planet would sit on an emissivity curve, it may be necessary to use complementary methods such as spectroscopy on the planet, to determine the atmospheric content, and therefore an estimate of the emissivity value.

In a similar vein, potential atmospheric clouds on an exoplanet can be important. Clouds may obscure the visibility of the planet, as was shown in simulations for JWST in Ref. [131]. This size of this effect will depend on the candidate being observed, and can substantially vary from planet to planet.

#### 3. Determining Exoplanet Ages

An independent age measurement of the exoplanet can certainly be a challenge in some circumstances. For brown dwarfs and Jupiters, while their temperature evolution curves are well known for a given mass and radius [58], it may be difficult to differentiate between a hot younger exoplanet, and an older DM-heated exoplanet. The age of a given exoplanet can in principle be estimated from its surroundings. For example, if it is in a bound system, it can be calibrated from its parent star. Brown dwarfs can often be in a binary system with another type of star, which can allow the age of brown dwarfs to be estimated from their companion star [137]. If it is a free-floating exoplanet, calibration is substantially more difficult, but can in principle be deduced from the age of any nearby systems in which it may have originated.

We expect overall that it will be difficult to resolve the age of all candidates, especially for planets at large distances. This could be due to, for example, no nearby system(s) that are easily enough identified as a rogue planet’s ejecting host, or due to the age uncertainties simply being too large. We expect, however, that the large

statistics that can be provided by these searches can form a sufficiently large dataset, which appears anomalous on average, given the expectations for the numerous systems studied. Conversely, and perhaps an easier task, is to find a sufficiently cold exoplanet, in contrast with the expectations of DM heating. This would allow a constraint on DM properties to be set.

#### 4. How Far Away Can We See DM-Heated Exoplanets?

The main source of signal degradation towards the GC is the number of stars present per pixel. This is because the number of stars increases dramatically, and these can overcrowd and outshine the exoplanet’s heat signal, making it impossible to detect. We now estimate how far into the GC we can observe a DM-heated exoplanet by comparing the expected stars-per-pixel with our regions of interest.

Comparing with known stellar densities [138], and taking a line of sight about 1 degree above the GC, the stellar mass is about  $2 \times 10^8 M_\odot$  per square degree. To convert this into a number of stars per square degree, we break the mass up into the fraction of expected mass in different types of stars. The stellar mass function is dominated by M-type stars contributing about 76% of the stellar population. We therefore expect about  $5 - 7 \times 10^8$  stars per square degree. Now, considering JWST’s NIRISS instrument, which provides our leading sensitivity towards the GC, we note that the field of view is 2.2 by 2.2 arcmin<sup>2</sup>. The NIRISS instrument has a single 2048 by 2048 pixel detector array with 65 milliarcsec pixels. This means there would be about  $5 - 7 \times 10^4$  stars in the field of view of JWST, and therefore that with NIRISS, we expect about 0.15 - 0.2 stars per pixel when observing about 1 degree above the GC. This means that, about 85% of the time, an exoplanet candidate at this distance could potentially be observed without any stars contaminating its pixel. We therefore expect that about 1 degree off the plane, that is, out to about 0.1 kpc, is required to collect large statistics for observing this signal. In principle, it may be possible to push this sensitivity further, at the cost of sacrificing statistics due to even further increased stellar crowding. The absolute sensitivity will be limited by the extremely dense region around the central black hole, with a radius of about 30 pc [139] – at this point, any observations are likely completely hopeless. We however present only 0.1 kpc in our results, as a more realistic sensitivity cutoff that may collect enough statistics.

Another important source of signal degradation can be dust extinction. This occurs when more dust is present, as it may absorb the light emitted from the exoplanet, or any other background star. Dust extinction is most prevalent for shorter wavelengths, where the scatter with cosmic dust is more likely. 2MASS has studied extinction in the *K*-band (near infrared) within 10 degrees of the GC [140]. The inner 0.5 degrees have very high dust extinction. For within 1 – 5 degrees, the south has 60

percent less extinction than the north, making it a better target. The south also features Baade’s window [141], which due to its low dust extinction allowed the SWEEPS exoplanets to be discovered. Near 1 degree, the dust extinction value in the *K*-band can be as low as  $A_K = 0.1$ , which will not significantly affect a signal in infrared, particularly not for temperatures between about 500 – 800 K.

We therefore expect, considering both the stars-per-pixel and dust extinction, above about 1 degree off the plane, that is, out to about 0.1 kpc, provides us with our maximum optimal expected JWST sensitivity. Of course, depending on the location of the candidate exoplanet, and the properties of the planet itself, elements of this search will vary. We expect that exoplanet experimentalists will be able to determine much more accurate results than the estimates we have presented here. However, we find that leading factors such as dust extinction and the background stellar numbers do not appear to completely conceal the potential DM-heating, by aiming for candidates off the plane, out to least 0.1 kpc. This is why we truncate our optimal sensitivity estimates in Fig. 1 and Fig. 3 at 0.1 kpc.

#### 5. Beyond JWST

It is possible that other telescopes may prove more fruitful than JWST in the future. While the current design of Roman has a red cutoff at 2.0 microns, it has been argued that extending the wavelength sensitivity further into the IR, by adding an *K*-filter to Roman, could allow infrared imaging of distant free-floating exoplanets [120], which due to its larger field of view and possible larger survey times, could potentially outperform JWST. It is also possible that Gaia Near Infra-Red (GaiaNIR), a proposed successor of Gaia in the near infrared, may improve this sensitivity, along with other potential future telescopes LUVUOIR or OST.

## V. DARK MATTER PARAMETER SPACE

We now consider the implications of DM-heated exoplanets for particle DM models. Mostly, limits from planetary heat flow investigate the parameter space of strongly interacting heavy DM candidates, so called SIMPs, see for example Refs. [40, 42]. We find that Jupiters and brown dwarfs are ideal laboratories to study light (sub-GeV) DM models with cross sections as small as a few picobarn. These exoplanets are advantageous over earth-like planets, as they can have large radii, high densities, and low core temperatures.



### A. DM Scattering and Capture

We parameterize the DM parameter space in terms of the DM mass and its elastic scattering cross sections with Standard Model (SM) particles. We will consider sensitivity to both DM-nucleon and DM-electron interactions.

For interactions with nucleons, we further distinguish two effective scenarios, a spin-independent scattering cross section with nucleons, and a spin-dependent scattering cross section. In the spin-independent cross section regime, given that our cross sections are small enough [142], we can write:

$$\sigma_{\chi A}^{\text{SI}} = \sigma_{\chi N}^{\text{SI}} \left( \frac{\mu(m_A)}{\mu(m_N)} \right)^2 \left[ Z + \frac{a_n}{a_p} (A - Z) \right]^2, \quad (13)$$

where  $m_A$  is the mass of the nucleus,  $m_N$  the nucleon mass,  $A$  the atomic number,  $\mu(m_A)$  and  $\mu(m_N)$  the DM-nucleus and DM-nucleon reduced masses respectively, and  $\sigma_{\chi N}^{\text{SI}}$  the DM-nucleon scattering cross section.

For the spin-dependent scattering cross section we have

$$\sigma_{\chi A}^{\text{SD}} = \sigma_{\chi N}^{\text{SD}} \left( \frac{\mu(m_A)}{\mu(m_N)} \right)^2 \frac{4(J+1)}{3J} [a_p \langle S_p \rangle + a_n \langle S_n \rangle]^2, \quad (14)$$

where  $J$  is the total nuclear spin,  $\langle S_p \rangle$  and  $\langle S_n \rangle$  the effective proton and neutron spins of the nucleus respectively, and  $a_p$  and  $a_n$  the model dependent DM-proton and DM-neutron coupling strength respectively. For our scenario only the couplings to protons will be relevant, since our targets are dominantly made of hydrogen and helium, and the latter has zero total nuclear spin. We assume  $a_p = 1$ .

To relate the DM heat flow in the previous sections with scattering cross sections, we need to find the range of parameters for which a fraction  $f$  of the DM particles passing through the planet is gravitationally captured. In order to determine the capture cross section, we adopt the formalism in Refs. [143, 144], that can take into account multiple DM scatterings inside an object. This formalism extends the calculations in Ref. [40] and is also valid in a regime where the escape velocity of the object exceeds the average DM velocity.

Normalizing to the maximal DM capture rate, we obtain the captured DM fraction

$$f = \frac{C_{\text{cap}}}{C_{\text{max}}} = \sum_{N=1}^{\infty} f_N, \quad (15)$$

with the capture fraction for a given number of scatterings being

$$f_N = p(N, \tau) \left[ 1 - \kappa \exp \left( -\frac{3(v_N^2 - v_{\text{esc}}^2)}{2v_d^2} \right) \right], \quad (16)$$

with

$$\kappa = \left( 1 + \frac{3v_N^2}{2v_d^2} \right) \left( 1 + \frac{3v_{\text{esc}}^2}{2v_d^2} \right)^{-1}. \quad (17)$$

Here  $v_d$  is the velocity dispersion,  $v_N = v_{\text{esc}}(1 - \langle z \rangle \beta)^{-N/2}$  where the average scattering angle is  $\langle z \rangle = 1/2$  [143],  $\beta = 4m_\chi m_A / (m_\chi + m_A)^2$ , and  $m_A$  is the mass of the target particle. The probability that the DM particle scatters  $N$  times is

$$p(N, \tau) = \frac{2}{\tau^2} \left( N_s + 1 - \frac{\Gamma(N_s + 2, \tau)}{N_s!} \right), \quad (18)$$

where  $\Gamma(a, b)$  is the incomplete gamma function. This scattering probability is a function of the optical depth,

$$\tau = \frac{3}{2} \frac{\sigma}{\sigma_{\text{sat}}}, \quad (19)$$

where  $\sigma_{\text{sat}} = \pi R^2 / N_{\text{SM}}$  is the saturation cross section,  $R$  the planetary radius,  $N_{\text{SM}}$  is the target particle number, and  $\sigma$  is the DM-target cross section.

In order to set sensitivity limits on DM scattering in Jupiters and brown dwarfs, we assume spheres of hydrogen with constant density. For reference, Jupiter contains about 84% hydrogen, and 16% helium [145]. To be conservative, we only consider the 84% hydrogen. As gas giants are expected to be dominated by these elements, we expect a hydrogen sphere (like Jupiter's composition) to be approximately representative. For the spin-independent limits, we conservatively neglect the potential enhancement by coherent scattering on molecular hydrogen, which would increase the cross section sensitivities by a factor 2 in some of the parameter space.

To obtain the limits on DM-electron scattering in exoplanets, we also assume a hydrogen sphere for the exoplanets. As the chemical composition is dominantly hydrogen, this allows the assumption that the proton number density is identical to the electron number density. A subdominant correction comes from the helium abundance, which we neglect to be conservative. Note that given the hydrogen target, relativistic shell effects play no role in the considered processes. We assume a momentum independent DM-electron cross section  $\sigma_{\chi e}$ , i.e. the electron form factor is  $F = 1$ .

We note that recently a refined simulation, taking the detailed propagation effects into account, showed how Earth and Mars' heat flow bounds improve for the multi-scatter regime [42]. We emphasize that in light of this improvement our cross section sensitivities are conservative; we do not perform such a simulation, which would simply strengthen our sensitivities. However, once specific candidates are known, the sensitivities may be refined with simulations incorporating the planetary composition in greater detail, which are outside the scope of this work.

### B. DM Evaporation

DM evaporation from the exoplanet truncates the low DM mass sensitivity. This is because if the kinetic energy of the thermalized DM particle exceeds the gravitational

potential, the DM will become unbounded again. This sets the orbit condition to remain bound, as

$$E_{\text{DM}}^{\text{kin}} = \frac{3}{2}T(r) < \frac{G_N M(r)m_\chi}{2r}, \quad (20)$$

where  $T(r)$  is the interior temperature of the exoplanet as a function of internal radius,  $G_N$  is the gravitational constant, and  $M(r)$  is the mass of the exoplanet enclosed within a given radius  $r$ . As we require that DM particles can accumulate in the cores of the objects in order to efficiently annihilate, we therefore require that the DM is bound to the exoplanet.

To compare with evaporation in Earth, we first take Earth density and temperature profiles [146]. For Earth, we find a minimum bounded DM mass of  $m_\chi^{\text{min}} = \mathcal{O}(100)$  MeV. Now, for Jupiter, with a core temperature of  $T_c = 1.5 \times 10^4$  K, an average density of  $\rho_{\text{jup}} = 1.3$  g/cm<sup>3</sup>, and a radius of  $R_{\text{jup}} = 6.99 \times 10^9$  cm, we have found the minimum bounded DM mass is  $m_\chi^{\text{min}} \sim 30$  MeV. This result applies to the exoplanet Jupiters, of comparable size. Note that we have checked two Jupiter density profile hypothesis, one with a core and the other without [121] and find no significant effect on the minimal DM mass.

For our brown dwarf benchmark point we use an analytical model as detailed in Sec. II. Compared to our cross section sensitivity estimates, where we assumed a hydrogen sphere, the evaporation limits require a model for the exoplanet core. The relatively low core temperatures and high densities make old brown dwarfs efficient accumulators for light DM. For our benchmark, the brown dwarf radius is taken to be  $R_{\text{BD}} = R_{\text{jup}}$ , and the mass  $M_{\text{BD}} = 75 M_{\text{jup}} = 0.07 M_\odot$ . This results in an average density of  $\rho_{\text{BD}} = 108$  g/cm<sup>3</sup>, a core density of  $\rho_c = 500$  g/cm<sup>3</sup> and a core temperature  $T_c = 2 \times 10^5$  K. The resulting minimal DM mass that does not evaporate in the brown dwarf is  $m_\chi^{\text{min}} \sim 3$  MeV.

Any other Jupiters, or Super Jupiters, will have a minimum exoplanet-bounded DM mass that is between the Jupiter benchmark (planetary mass  $M_{\text{jup}}$ ), and the brown dwarf benchmark (planetary mass  $75 M_{\text{jup}}$ ). The DM mass where evaporation occurs will depend on where the mass of the exoplanet in question sits relevant to these benchmarks.

### C. DM Equilibration

DM capture and annihilation must reach equilibrium in order for the heating process to be maximally effective [147]. In this subsection, we show equilibrium can be expected to be reached in our exoplanets of interest. As our sensitivity extends into the sub-GeV regime (as shown above with lower evaporation masses), we consider both the standard  $2 \rightarrow 2$  annihilation process, as well as  $3 \rightarrow 2$  annihilation processes, which can be key for light DM.

#### 1. $\chi\chi \rightarrow SM + SM$ Annihilation Processes

For a DM candidate that annihilates via a  $2 \rightarrow 2$  process to SM particles, the annihilation rate is given by the volume integral

$$\Gamma_{\text{ann}}^{2 \rightarrow 2} = \int dV n_\chi^2 \langle \sigma_{\text{ann}} v_{\text{rel}} \rangle, \quad (21)$$

where  $n_\chi$  is the DM number density, and  $\langle \sigma_{\text{ann}} v_{\text{rel}} \rangle$  is the thermal averaged cross section, with  $\sigma_{\text{ann}}$  the annihilation cross section, and  $v_{\text{rel}}$  the relative DM velocity.

The equilibrium number of DM particles in the object is found from the solution of the differential equation

$$\dot{N}_\chi = C_{\text{cap}} - C_{\text{evap}} N_\chi - C_{\text{ann}}^{2 \rightarrow 2} N_\chi^2, \quad (22)$$

where  $N_\chi$  is the DM number,  $C_{\text{cap}}$  is the capture rate,  $C_{\text{evap}}$  the evaporation rate, and the annihilation coefficient is given by

$$C_{\text{ann}}^{2 \rightarrow 2} = \langle \sigma_{\text{ann}} v_{\text{rel}} \rangle / V_{\text{eff}}^{2 \rightarrow 2}. \quad (23)$$

The annihilation volume is  $V_{\text{eff}}^{2 \rightarrow 2} = V_1^2 / V_2$ , with the volume for a given species  $j$  being

$$V_j = 4\pi \int_0^R e^{-j m_\chi \phi(r)/T(r)} r^2 dr. \quad (24)$$

Here,  $R$  is the radius of the exoplanet,  $T(r)$  is the planetary interior temperature as a function of radius,  $\phi(r)$  is the gravitational potential, and  $r$  is the radius of the volume within the exoplanet. The equilibration time scale is then given by

$$\tau = (C_{\text{ann}} C_{\text{cap}})^{-1/2}. \quad (25)$$

This can be converted into a lower bound on the annihilation cross section,

$$\langle \sigma_{\text{ann}} v_{\text{rel}} \rangle \geq V_{\text{eff}}^{2 \rightarrow 2} / (C_{\text{cap}} \tau^2). \quad (26)$$

Compared to Earth, Jupiters have an effective volume of the order of  $V_{\text{eff}}^{\text{Jupiters}} \sim \mathcal{O}(100) V_{\text{eff}}^{\text{Earth}}$ , and equilibration times of about  $\tau \sim 10$  Gyr are feasible, in contrast to Earth, where  $\tau \sim 1$  Gyr is assumed. Since the minimal annihilation cross section required for equilibration scales linearly with the effective volume, and with the inverse square of the equilibration time, the above rescaling leaves the equilibration criterion invariant. Thus, like Earth, we have for Jupiters,  $\langle \sigma_{\text{ann}} v_{\text{rel}} \rangle \geq 10^{-30} (m_\chi/\text{GeV})^{-1} \text{ cm}^3/\text{s}$ , which is expected to be satisfied in models with a thermal freezeout.

#### 2. $\chi + \chi + \chi \rightarrow \chi + \chi$ Annihilation Processes

As our searches focus on the sub-GeV regime, now we discuss models of light, thermally produced DM, which are based on  $3 \rightarrow 2$  interactions. In a broad class of

models, suggested in Ref. [148], the DM freezes out via the interaction  $\chi + \chi + \chi \rightarrow \chi + \chi$ . The freezeout condition for the interaction rate factor is then  $\langle \sigma_{3 \rightarrow 2} v_{\text{rel}}^2 \rangle = 10^8 (m_\chi/\text{GeV})^{-1} \text{GeV}^{-5}$  [149]. The corresponding annihilation rate in planets is given by the volume integral

$$\Gamma_{\text{ann}}^{3 \rightarrow 2} = \int dV n_\chi^3 \langle \sigma_{3 \rightarrow 2} v_{\text{rel}}^2 \rangle, \quad (27)$$

resulting in an annihilation rate of

$$C_{\text{ann}}^{3 \rightarrow 2} = \langle \sigma_{3 \rightarrow 2} v_{\text{rel}}^2 \rangle / (V_{\text{eff}}^{3 \rightarrow 2})^2, \quad (28)$$

with an annihilation volume of  $V_{\text{eff}}^{3 \rightarrow 2} = V_1 \sqrt{V_1/V_3}$ . The equilibrium condition on the rate factor then reads

$$\langle \sigma_{3 \rightarrow 2} v_{\text{rel}}^2 \rangle \geq (V_{\text{eff}}^{3 \rightarrow 2})^2 / (C_{\text{cap}} \tau^2). \quad (29)$$

Given a Jupiter-like planet with  $M = M_{\text{jup}}$ ,  $R = R_{\text{jup}}$  and  $\tau = 10 \text{ Gyr}$ , this gives

$$\langle \sigma_{3 \rightarrow 2} v_{\text{rel}}^2 \rangle \geq 10^{51} (m_\chi/\text{GeV}) \text{GeV}^{-5}, \quad (30)$$

which is many orders of magnitude larger than the value expected from the thermal freezeout. This means that the  $\chi + \chi + \chi \rightarrow \chi + \chi$  process does not reach equilibrium in sufficient time. There is however, another  $3 \rightarrow 2$  process that can be relevant, which we now discuss.

### 3. $\chi + \chi + SM \rightarrow \chi + SM$ Annihilation Processes

Recently, a different number changing interaction has been proposed in order to produce light, thermal DM, called the Co-SIMP [155]. In this scenario, the DM freeze-out is assisted by SM particles, in the process  $\chi + \chi + SM \rightarrow \chi + SM$ . Since the number density of SM particles in a planet is by many orders of magnitude larger than the accumulated DM number density, this interaction rate is significantly more efficient. This leads to a prediction for the rate factor,  $\langle \sigma_{3 \rightarrow 2} v_{\text{rel}}^2 \rangle = 10^3 (m_\chi/\text{GeV})^{-3} \text{GeV}^{-5}$ . The annihilation rate in exoplanets is given by

$$\Gamma_{\text{ann}}^{3 \rightarrow 2} = \int dV n_\chi^2 n_{\text{SM}} \langle \sigma_{3 \rightarrow 2} v_{\text{rel}}^2 \rangle, \quad (31)$$

resulting in an annihilation rate of

$$C_{\text{ann}}^{3 \rightarrow 2} = \langle \sigma_{3 \rightarrow 2} v_{\text{rel}}^2 \rangle n_{\text{SM}} / V_{\text{eff}}^{2 \rightarrow 2}, \quad (32)$$

with the condition that

$$\langle \sigma_{3 \rightarrow 2} v_{\text{rel}}^2 \rangle \geq V_{\text{eff}}^{2 \rightarrow 2} / (\tau^2 C_{\text{cap}} n_{\text{SM}}). \quad (33)$$

For a Jupiter-like planet, this gives a minimum rate to reach equilibrium,

$$\langle \sigma_{3 \rightarrow 2} v_{\text{rel}}^2 \rangle \geq 10^{-2} (m_\chi/\text{GeV}) \text{GeV}^{-5}. \quad (34)$$

This is well below the thermally expected rate, such that captured Co-SIMP particles always reach equilibrium.

As we consider elastic cross sections that lead to all the outgoing particles becoming trapped in the planet, this means that the entire mass energy released in the Co-SIMP process will be converted to the planetary heat flow.

In fact, this process is even more broadly applicable. In Ref. [148], it is shown that in the SIMP model the Co-SIMP process exists, however, the rate is suppressed by a factor  $\epsilon^2$ . Experimentally this quantity is constrained to be in the range of  $\epsilon \sim 10^{-6} - 10^{-8}$ , and therefore the Co-SIMP process will be subdominant to the thermal SIMP rate. Regardless, the subdominant Co-SIMP process will still be the process that brings the particles into annihilation equilibrium (as opposed to kinetic equilibrium that only equilibrates the temperatures), due to the larger number density. We therefore expect that the Jupiters and brown dwarf searches will probe new territory of the number changing, thermal DM models.

## D. DM Cross Section Sensitivities

Figure 6 shows our sensitivity estimates for Jupiter-like planets and brown dwarfs to the DM parameter space for the spin-dependent and spin-independent DM-nucleon scattering. Note that the scattering sensitivity arises predominately from DM-proton interactions. This is because gas giants and brown dwarfs are predominately hydrogen and helium; hydrogen only has a proton, and helium has zero total nuclear spin, thus DM-neutron interactions are not significant. For both Jupiters and brown dwarfs, we show sensitivity to the both the maximum capture rate (for which all DM is captured, and planets are maximally heated), as well as a 10% DM capture rate (which causes less heating, but still may be detectable). These sensitivities do not specifically depend on the DM density profile or DM density value; sensitivity to the cross sections shown only requires that the DM-heating temperature has exceeded the internal heating temperature for the relevant target exoplanet. We show the earth heat flow bounds from Ref. [42] for comparison, and direct detection bounds [156, 157]. In the case of spin-independent scattering, the sensitivity of direct detection experiments to light DM can be enhanced by taking into account boosts from collisions with cosmic rays [154, 158–160], which are shown in the top regions of the plots.

Figure 7 shows the DM-electron scattering sensitivity estimates, alongside existing limits from direct detection [161–172] and solar reflection [173, 174]. While the region of sensitivity of Jovian planets is already constrained by direct detection experiments, brown dwarfs will have some sensitivity to new DM-electron scattering parameter space. We show the sensitivity for when 100% and 10% of DM is captured. Electron-dominated interactions may be found in for example leptophilic DM models [175–179].

For both Fig. 6 and Fig. 7, the sensitivity region would

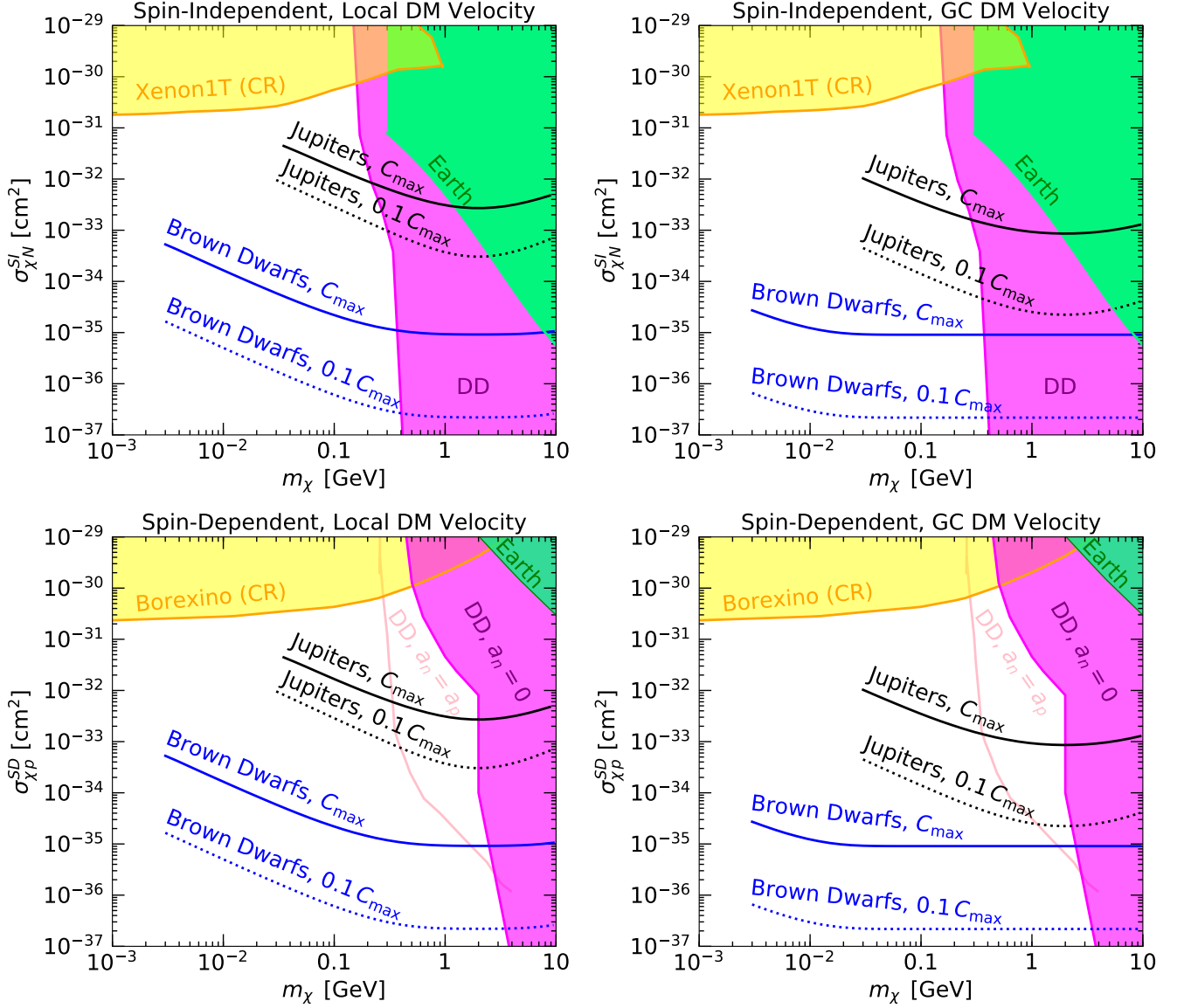


Figure 6. Spin-independent (top row) and spin-dependent (bottom row) DM-nucleon scattering cross section sensitivity estimates for Jupiters and brown dwarfs, for exoplanets in a local DM velocity (left column) or GC DM velocity (right column) calculated in this work. The solid lines show cross sections assuming 100% of incoming DM is captured ( $C_{\max}$ ), and the dotted lines show cross sections for when 10% of DM is captured ( $0.1 C_{\max}$ ). Complementary constraints are also shown; Earth is the limit on Earth DM-heat flow [42], DD is a collection of direct detection experiments [150–153], Xenon1T (CR) [154] and Borexino (CR) [154] correspond to cosmic-ray boosted DM signals. For spin-dependent scattering, two different DD bounds are shown; if the proton  $a_p$  and neutron  $a_n$  couplings are equal, the light pink line would be filled, if the neutron coupling  $a_n$  is zero, the magenta shaded region is the DD limit (the exoplanet limits are not affected by this choice).

be all filled in as a constraint if a sufficiently cold Jupiter or brown dwarf were measured. For instead discovery of a DM-heating signal, the DM parameters would lie above the dashed lines shown. As both these figures show 100% and 10% values of the DM capture rate, in principle even stronger sensitivity to DM cross sections can be reached if an even smaller DM capture fraction can be probed. However, given the JWST optimal sensitivity, about a 10% DM capture fraction is likely the smallest capture fraction that can be probed in the near future.

Note that there is a ceiling for the cross sections above which the DM does not drift fast enough into the planet’s core [180]. However, even in the case of a dense brown dwarf, and sub-GeV DM masses, we find that this ceiling is of the order of  $\sigma_{\max} \sim 10^{-25}$  cm<sup>2</sup> (for the sub-GeV DM mass range). Such cross section values are at the threshold where a point-like DM description is barely valid, and another physical description for DM must be used. Importantly, brown dwarfs provide complementary sensitivity to parameter space that can be tested by CR boosted



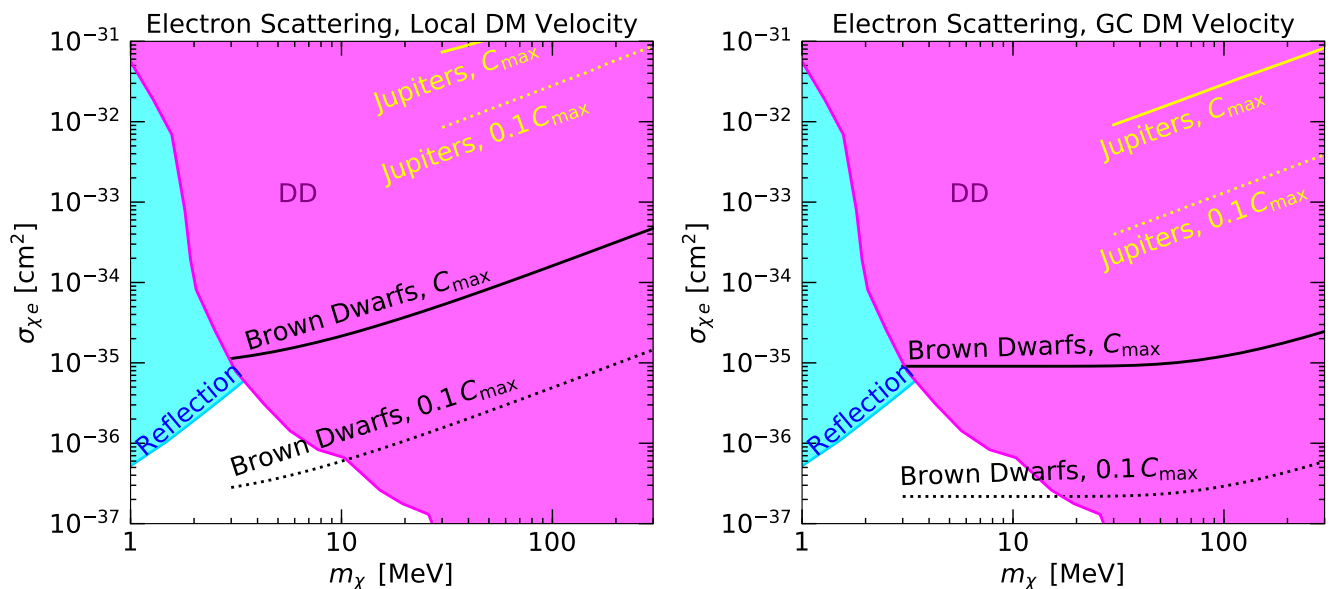


Figure 7. DM-electron scattering cross section sensitivity for brown dwarfs and Jupiters, for exoplanets in a local DM velocity (left) or GC DM velocity (right) calculated in this work. The solid lines show sensitivity assuming 100% of incoming DM is captured ( $C_{\max}$ ), and the dotted lines show sensitivity for when 10% of DM is captured ( $0.1 C_{\max}$ ). Complementary constraints from direct detection (DD) [161–172] and solar reflection [173] are shown.

DM, which can be difficult to interpret owing to no-energy dependence being used, despite being high-energy processes. Note that while we have cast our sensitivity in terms of one DM particle with one interaction type, in principle several particle processes may be present in the dark sector, which can alter the expected phenomenology (see e.g. Refs [181–186]). Detailed model-dependent studies would need to be performed to determine the full range of particle physics possibilities. Importantly, note that direct detection or other competing bounds may be weakened or removed in some DM models, while the exoplanet sensitivities would remain present. This can be true, for example, in inelastic DM models.

In order to contribute significantly to the heat flow, the DM population should have a dominant symmetric component (and not dominantly annihilate into invisible final states), which is a natural outcome in scenarios with thermally produced DM. Thermally produced DM candidates, with sub-GeV masses are known to exist in models with light mediators [187] and production mechanisms with number changing interactions [148, 155]. As discussed in detail in Ref. [187], DM models with dominant interactions with nucleons, and  $m_\chi < \text{GeV}$  face severe experimental constraints if their thermal abundance is set by a  $2 \rightarrow 2$  freezeout process. However, in this case it is possible that their abundance may be set by a number changing process [148, 155]. On the other hand, if the DM primarily interacts with leptons, both a freeze-in production [187] and a WIMP-like  $2 \rightarrow 2$  freezeout production process [173] are experimentally allowed for sub-GeV masses. We re-emphasize that the sensitivities do not scale linearly with the DM density profiles. If ex-

perimentally an exoplanet in a given class is found with a temperature lower than the predicted value, the entire mass-cross section region is immediately excluded.

## VI. SUMMARY AND CONCLUSIONS

The exoplanet program is rapidly accelerating. Amongst the billions of new worlds in our Galaxy, many are waiting to reveal their surprises. Unexpected discoveries are inevitable, and numerous new telescopes with cutting-edge technology are ready to make them. In this work, we have examined how exoplanets can be used to discover DM or other new physics. For the first time, we have pointed out the broad applicability of exoplanets to be used as DM detectors, with actionable discovery or exclusion searches using new infrared telescopes. We target old, cold, Jupiter-like planets and brown dwarfs, which are particularly advantageous due to their large sizes, densities, and low core temperatures.

Our first suggested search can be expected to bring shorter-term results. There are hundreds of known Jupiters in our local neighborhood, and Gaia is expected to identify tens of thousands of potential candidates in the next few years. These collectively provide an enormous statistical sample for a DM-heated exoplanet search. We identified numerous known exoplanets as candidates for this search, and estimated the JWST sensitivity to their potential planetary temperatures. We concluded that local searches show strong promise to discover DM-heated planets. If no DM-heating signal is found, new constraints can be set on the DM mass and

scattering rate.

Our second suggested search is more ambitious, but may be fruitful simply due to the enormous number of exoplanets in our Galaxy. We pointed out that the exoplanet temperature is expected to be correlated with DM density, rising sharply towards the GC. This leads to a new DM search; by brute statistical force, we may be able to discover DM by measuring DM-density-correlated heated exoplanets. The presence of DM overdensities or substructure may also be confirmed with exoplanets, with a pocket of even hotter DM-heated exoplanets. Alternatively, the larger expected DM-heating signal in these DM overdensities can lead to even stronger constraints, if exoplanets are measured to be sufficiently cold.

We estimated the impact of difficulties in seeing a DM-heated exoplanet at such large distances into the GC. We found that stellar crowding was the main limiting factor, and that dust extinction was minimal at the infrared wavelengths and galactic locations of interest. We determined that to minimize both dust extinction and stellar crowding, and maximize a potential DM-heating signature, the optimal distance for a candidate exoplanet is about 0.1 kpc off the plane. We also noted that, in order to measure exoplanet temperatures at such large distances, the exoplanet must be a rogue planet. Otherwise, it cannot be resolved from a parent star, and would be greatly outshone. We concluded that, at an estimate, JWST may have sensitivity to exoplanet temperatures above about 650 K, for exoplanets all the way into about 0.1 kpc of the inner Galaxy (for more local searches, the minimum temperature sensitivity is of course lower). While this search may be challenging, we again emphasize the large statistics that may be available with the many exoplanet telescopes that are upcoming or are currently being proposed. As per the local search, if a sufficiently cold exoplanet is discovered, this would allow a constraint to be set on the DM mass and scattering cross section.

We calculated the DM parameter space sensitivity to brown dwarfs and Jupiters that may have their temperature measured in the near future. We determined that DM with masses above about an MeV can be probed with exoplanets, with DM-proton and DM-electron scattering cross sections down to about  $10^{-37}$  cm<sup>2</sup>, stronger than some existing limits by up to six orders of magnitude. We pointed out that this DM mass sensitivity is lighter than many other celestial body searches for DM heat flow. This is because brown dwarfs and Jupiters have large integrated column densities, and given the ratio between the gravitational potential and the core temperature, it is more difficult for light DM to evaporate in these systems. Interestingly, we found that new processes also become relevant in this previously unprobed sub-GeV DM-heating regime. In particular, we found that certain  $3 \rightarrow 2$  annihilation processes can be vital to ensure that equilibrium is reached for sub-GeV DM.

Going forward, it will be important to investigate in more detail the impact of DM in stellar or planetary sys-

tems. Detailed simulations of temperature curves as a function of age for brown dwarfs or Jupiters, when DM heating is present and taking into account several planetary effects, will be required to make more precise statements than the estimates presented in this work. More broadly, we also emphasize that it may not be valid to calculate a planet’s age based on its temperature alone, as is often done in the literature. This is because, as we have shown, DM heating can increase exoplanet temperatures, providing a departure from the standard age-cooling curves.

The question of whether we are alone in the Universe has sparked an explosion of interest for a planet like our own. The exoplanet search program is accelerating, and we can expect many more planets to be found soon. New infrared telescopes such as JWST will be sensitive to DM induced exoplanet heating, providing us a new infrared window into DM in our local neighborhood, and DM dense regions at the heart of our Galaxy.

## ACKNOWLEDGMENTS

We thank John Beacom, Joe Bramante, Chris Cappiello, Rouven Essig, Katie Freese, Savannah Jacklin, Shirley Li, Nirmal Raj, Pat Scott, Sara Seager, Aaron Vincent, and Ji Wang for helpful comments and discussions. RKL was supported by the Office of High Energy Physics of the U.S. Department of Energy under Grant No. DE-SC00012567 and DE-SC0013999, as well as the NASA Fermi Guest Investigator Program under Grant No. 80NSSC19K1515, and later at SLAC under Contract DE-AC02-76SF00515. J.S. is largely supported by a Feodor Lynen Fellowship from the Alexander von Humboldt foundation.

## Appendix A: Impact of Atmospheric Emissivity

Exoplanet atmospheric emissivity can have an impact on JWST searches. This is because emissivity can trap some exoplanet heat flow, leading to higher temperatures. We now briefly demonstrate how this can improve JWST sensitivities.

Figure 8 (left) shows the impact of varied exoplanet emissivity on the spectral flux density. As the internal heat and the power output of a planet is a conserved quantity, a higher temperature can be obtained for smaller emissivity values, at the cost of a drop in the normalization of the spectral flux. As energy is conserved, this leads to the *same* total integrated flux for all emissivities, but the temperature peaks at a shorter wavelength. The main benefit is therefore being able to exploit the more powerful filters available on JWST’s instruments; longer wavelengths generally have worse flux sensitivity than the shorter wavelengths. The example scenario shown here is for a DM-heated Jupiter at 10

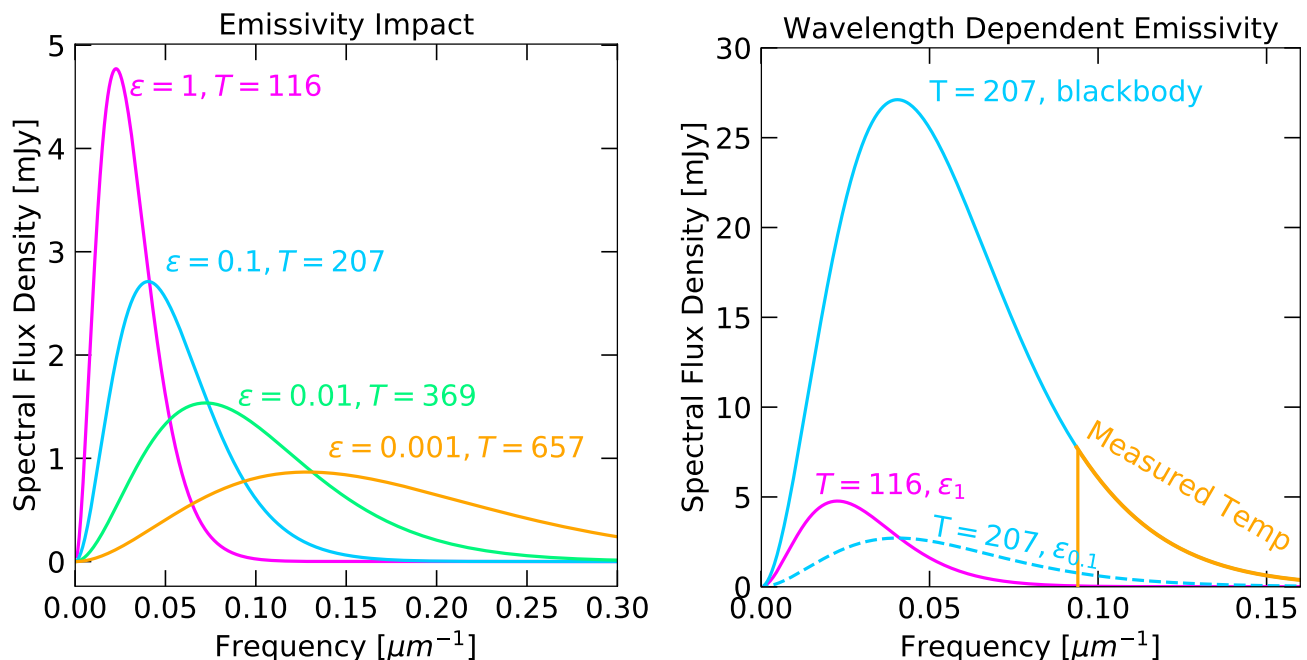


Figure 8. Impact of atmospheric emissivity on heating signals. **Left:** Temperature peak shifts for smaller emissivities. **Right:** Schematic example of wavelength-dependent emissivity values, which can substantially boost signal intensity. This example has emissivity of one above about  $0.08 \mu\text{m}^{-1}$ , and very suppressed emissivities below this frequency. This leads to a non-suppressed peak at higher frequencies, shown as the orange “measured temp” curve. The non-suppressed version of the emissivity equal to 0.1 curve is shown in solid blue. The dashed blue is the correctly rescaled version of the emissivity 0.1 case (i.e., the 0.1 penalty is applied to the blackbody temperature). The emissivity equal to one case is shown as solid magenta.

pc, which is a slice at  $d = 10$  pc through Fig. 4. While an increased emissivity can lead to a larger effect also for the longer-distance searches, the effect is generally not as pronounced, as the higher temperature filters are not substantially more powerful than the already high-temperature filters used at large distances in the  $\epsilon = 1$  case shown in Fig. 3.

Figure 8 (right) shows a schematic wavelength-dependent emissivity scenario. Indeed, in reality, an exoplanet may have different emissivities at different wavelengths, due to some wavelengths being better reflected by the atmosphere. For example, one could imagine an atmosphere leaving optical wavelengths mostly unaffected, while internally reflecting infrared wavelengths. This would lead to an extreme departure from the usual blackbody spectrum, similar to what is shown in the right figure. This also can allow both a boost in flux density compared to an emissivity value that is constant at all wavelengths, as well as applicability of better filters at shorter wavelengths. A planet could look, for example, truly like a higher temperature planet if only observing

the edge of the spectrum (e.g. if a telescope was wavelength limited), without decreased normalization, while in other wavelengths, the normalization could be greatly suppressed due to the emissivity factor. In such a scenario, the area under the curves would still be conserved (e.g. the area under all of the smaller three fluxes in Fig. 8 is conserved). This variance of temperature peaks, at different emissivities, when the planet could not otherwise reach such high temperatures without DM, would be a smoking gun signal of a DM-heated planet. To be conservative, we do not use wavelength-dependent emissivities in our main results; we only point out this can potentially considerably boost sensitivities.

Lastly, note that at small emissivity values, the exoplanet surface temperature might become completely unaccessible, and DM-heating may instead only impact the temperature of the atmosphere in an energy exchange process. The details of such an effect will however depend on the exoplanet in question, and is an interesting possibility to study in a dedicated simulation, which is outside the scope of this work.

[1] I. Goldman and S. Nussinov, “Weakly Interacting Massive Particles and Neutron Stars,” *Phys. Rev.* **D40**, 3221–3230 (1989).

[2] Andrew Gould, Bruce T. Draine, Roger W. Romani, and Shmuel Nussinov, “Neutron Stars: Graveyard of Charged Dark Matter,” *Phys. Lett.* **B238**, 337–343

- (1990).
- [3] Chris Kouvaris, “WIMP Annihilation and Cooling of Neutron Stars,” *Phys. Rev.* **D77**, 023006 (2008), [arXiv:0708.2362 \[astro-ph\]](#).
  - [4] Gianfranco Bertone and Malcolm Fairbairn, “Compact Stars as Dark Matter Probes,” *Phys. Rev.* **D77**, 043515 (2008), [arXiv:0709.1485 \[astro-ph\]](#).
  - [5] Arnaud de Lavallaz and Malcolm Fairbairn, “Neutron Stars as Dark Matter Probes,” *Phys. Rev.* **D81**, 123521 (2010), [arXiv:1004.0629 \[astro-ph.GA\]](#).
  - [6] Chris Kouvaris and Peter Tinyakov, “Can Neutron stars constrain Dark Matter?” *Phys. Rev.* **D82**, 063531 (2010), [arXiv:1004.0586 \[astro-ph.GA\]](#).
  - [7] Samuel D. McDermott, Hai-Bo Yu, and Kathryn M. Zurek, “Constraints on Scalar Asymmetric Dark Matter from Black Hole Formation in Neutron Stars,” *Phys. Rev.* **D85**, 023519 (2012), [arXiv:1103.5472 \[hep-ph\]](#).
  - [8] Chris Kouvaris and Peter Tinyakov, “Excluding Light Asymmetric Bosonic Dark Matter,” *Phys. Rev. Lett.* **107**, 091301 (2011), [arXiv:1104.0382 \[astro-ph.CO\]](#).
  - [9] Tolga Guver, Arif Emre Erkoca, Mary Hall Reno, and Ina Sarcevic, “On the capture of dark matter by neutron stars,” *JCAP* **1405**, 013 (2014), [arXiv:1201.2400 \[hep-ph\]](#).
  - [10] Joseph Bramante, Keita Fukushima, and Jason Kumar, “Constraints on bosonic dark matter from observation of old neutron stars,” *Phys. Rev.* **D87**, 055012 (2013), [arXiv:1301.0036 \[hep-ph\]](#).
  - [11] Nicole F. Bell, Andrew Melatos, and Kalliopi Petraki, “Realistic neutron star constraints on bosonic asymmetric dark matter,” *Phys. Rev.* **D87**, 123507 (2013), [arXiv:1301.6811 \[hep-ph\]](#).
  - [12] Joseph Bramante, Keita Fukushima, Jason Kumar, and Elan Stopnitzky, “Bounds on self-interacting fermion dark matter from observations of old neutron stars,” *Phys. Rev.* **D89**, 015010 (2014), [arXiv:1310.3509 \[hep-ph\]](#).
  - [13] Bridget Bertoni, Ann E. Nelson, and Sanjay Reddy, “Dark Matter Thermalization in Neutron Stars,” *Phys. Rev.* **D88**, 123505 (2013), [arXiv:1309.1721 \[hep-ph\]](#).
  - [14] Chris Kouvaris and Peter Tinyakov, “Constraining Asymmetric Dark Matter through observations of compact stars,” *Phys. Rev.* **D83**, 083512 (2011), [arXiv:1012.2039 \[astro-ph.HE\]](#).
  - [15] Matthew McCullough and Malcolm Fairbairn, “Capture of Inelastic Dark Matter in White Dwarves,” *Phys. Rev.* **D81**, 083520 (2010), [arXiv:1001.2737 \[hep-ph\]](#).
  - [16] M. Angeles Perez-Garcia and Joseph Silk, “Constraining decaying dark matter with neutron stars,” *Phys. Lett.* **B744**, 13–17 (2015), [arXiv:1403.6111 \[astro-ph.SR\]](#).
  - [17] Joseph Bramante, “Dark matter ignition of type Ia supernovae,” *Phys. Rev. Lett.* **115**, 141301 (2015), [arXiv:1505.07464 \[hep-ph\]](#).
  - [18] Peter W. Graham, Surjeet Rajendran, and Jaime Varela, “Dark Matter Triggers of Supernovae,” *Phys. Rev.* **D92**, 063007 (2015), [arXiv:1505.04444 \[hep-ph\]](#).
  - [19] Marina Cermeneno, M. Angeles Perez-Garcia, and Joseph Silk, “Light dark matter scattering in outer neutron star crusts,” *Phys. Rev.* **D94**, 063001 (2016), [arXiv:1607.06815 \[astro-ph.HE\]](#).
  - [20] Peter W. Graham, Ryan Janish, Vijay Narayan, Surjeet Rajendran, and Paul Riggins, “White Dwarfs as Dark Matter Detectors,” *Phys. Rev.* **D98**, 115027 (2018), [arXiv:1805.07381 \[hep-ph\]](#).
  - [21] Javier F. Acevedo and Joseph Bramante, “Supernovae Sparked By Dark Matter in White Dwarfs,” *Phys. Rev.* **D100**, 043020 (2019), [arXiv:1904.11993 \[hep-ph\]](#).
  - [22] Ryan Janish, Vijay Narayan, and Paul Riggins, “Type Ia supernovae from dark matter core collapse,” *Phys. Rev.* **D100**, 035008 (2019), [arXiv:1905.00395 \[hep-ph\]](#).
  - [23] Rebecca Krall and Matthew Reece, “Last Electroweak WIMP Standing: Pseudo-Dirac Higgsino Status and Compact Stars as Future Probes,” *Chin. Phys.* **C42**, 043105 (2018), [arXiv:1705.04843 \[hep-ph\]](#).
  - [24] David McKeen, Ann E. Nelson, Sanjay Reddy, and Dake Zhou, “Neutron stars exclude light dark baryons,” *Phys. Rev. Lett.* **121**, 061802 (2018), [arXiv:1802.08244 \[hep-ph\]](#).
  - [25] Masha Baryakhtar, Joseph Bramante, Shirley Weishi Li, Tim Linden, and Nirmal Raj, “Dark Kinetic Heating of Neutron Stars and An Infrared Window On WIMPs, SIMPs, and Pure Higgsinos,” *Phys. Rev. Lett.* **119**, 131801 (2017), [arXiv:1704.01577 \[hep-ph\]](#).
  - [26] Nirmal Raj, Philip Tanedo, and Hai-Bo Yu, “Neutron stars at the dark matter direct detection frontier,” *Phys. Rev.* **D97**, 043006 (2018), [arXiv:1707.09442 \[hep-ph\]](#).
  - [27] Nicole F. Bell, Giorgio Busoni, and Sandra Robles, “Heating up Neutron Stars with Inelastic Dark Matter,” *JCAP* **1809**, 018 (2018), [arXiv:1807.02840 \[hep-ph\]](#).
  - [28] Raghuvveer Garani, Yoann Genolini, and Thomas Hambye, “New Analysis of Neutron Star Constraints on Asymmetric Dark Matter,” *JCAP* **1905**, 035 (2019), [arXiv:1812.08773 \[hep-ph\]](#).
  - [29] Chian-Shu Chen and Yen-Hsun Lin, “Reheating neutron stars with the annihilation of self-interacting dark matter,” *JHEP* **08**, 069 (2018), [arXiv:1804.03409 \[hep-ph\]](#).
  - [30] Basudeb Dasgupta, Aritra Gupta, and Anupam Ray, “Dark matter capture in celestial objects: Improved treatment of multiple scattering and updated constraints from white dwarfs,” *JCAP* **08**, 018 (2019), [arXiv:1906.04204 \[hep-ph\]](#).
  - [31] Koichi Hamaguchi, Natsumi Nagata, and Keisuke Yanagi, “Dark Matter Heating vs. Rotochemical Heating in Old Neutron Stars,” *Phys. Lett.* **B795**, 484–489 (2019), [arXiv:1905.02991 \[hep-ph\]](#).
  - [32] Daniel A. Camargo, Farinaldo S. Queiroz, and Riccardo Sturani, “Detecting Dark Matter with Neutron Star Spectroscopy,” *JCAP* **1909**, 051 (2019), [arXiv:1901.05474 \[hep-ph\]](#).
  - [33] Nicole F. Bell, Giorgio Busoni, and Sandra Robles, “Capture of Leptophilic Dark Matter in Neutron Stars,” *JCAP* **1906**, 054 (2019), [arXiv:1904.09803 \[hep-ph\]](#).
  - [34] Raghuvveer Garani and Julian Heeck, “Dark matter interactions with muons in neutron stars,” *Phys. Rev.* **D100**, 035039 (2019), [arXiv:1906.10145 \[hep-ph\]](#).
  - [35] Javier F. Acevedo, Joseph Bramante, Rebecca K. Leane, and Nirmal Raj, “Warming Nuclear Pasta with Dark Matter: Kinetic and Annihilation Heating of Neutron Star Crusts,” *JCAP* **03**, 038 (2020), [arXiv:1911.06334 \[hep-ph\]](#).
  - [36] Aniket Joglekar, Nirmal Raj, Philip Tanedo, and Hai-Bo Yu, “Relativistic capture of dark matter by electrons in neutron stars,” (2019), [arXiv:1911.13293 \[hep-ph\]](#).
  - [37] Aniket Joglekar, Nirmal Raj, Philip Tanedo, and Hai-Bo Yu, “Kinetic Heating from Contact Interactions with Relativistic Targets: Electrons Capture Dark Matter in Neutron Stars,” (2020), [arXiv:2004.09539 \[hep-ph\]](#).
  - [38] Nicole F. Bell, Giorgio Busoni, Sandra Robles, and



- Michael Virgato, “Improved Treatment of Dark Matter Capture in Neutron Stars,” (2020), [arXiv:2004.14888 \[hep-ph\]](#).
- [39] Basudeb Dasgupta, Aritra Gupta, and Anupam Ray, “Dark matter capture in celestial objects: light mediators, self-interactions, and complementarity with direct detection,” (2020), [arXiv:2006.10773 \[hep-ph\]](#).
- [40] Gregory D. Mack, John F. Beacom, and Gianfranco Bertone, “Towards Closing the Window on Strongly Interacting Dark Matter: Far-Reaching Constraints from Earth’s Heat Flow,” *Phys. Rev. D* **76**, 043523 (2007), [arXiv:0705.4298 \[astro-ph\]](#).
- [41] Bhavesh Chauhan and Subhendra Mohanty, “Constraints on leptophilic light dark matter from internal heat flux of Earth,” *Phys. Rev. D* **94**, 035024 (2016), [arXiv:1603.06350 \[hep-ph\]](#).
- [42] Joseph Bramante, Andrew Buchanan, Alan Goodman, and Eesha Lodhi, “Terrestrial and Martian Heat Flow Limits on Dark Matter,” *Phys. Rev. D* **101**, 043001 (2020), [arXiv:1909.11683 \[hep-ph\]](#).
- [43] Saibal Mitra, “Uranus’ anomalously low excess heat constrains strongly interacting dark matter,” *Phys. Rev. D* **70**, 103517 (2004), [arXiv:astro-ph/0408341](#).
- [44] Stephen L. Adler, “Planet-bound dark matter and the internal heat of Uranus, Neptune, and hot-Jupiter exoplanets,” *Phys. Lett. B* **671**, 203–206 (2009), [arXiv:0808.2823 \[astro-ph\]](#).
- [45] M. Kawasaki, H. Murayama, and T. Yanagida, “Can the strongly interacting dark matter be a heating source of Jupiter?” *Prog. Theor. Phys.* **87**, 685–692 (1992).
- [46] Raghuvveer Garani and Peter Tinyakov, “Constraints on Dark Matter from the Moon,” *Phys. Lett. B* **804**, 135403 (2020), [arXiv:1912.00443 \[hep-ph\]](#).
- [47] Man Ho Chan and Chak Man Lee, “Constraining the spin-independent elastic scattering cross section of dark matter using the Moon as a detection target and the background neutrino data,” *Phys. Rev. D* **102**, 023024 (2020), [arXiv:2007.01589 \[astro-ph.HE\]](#).
- [48] Samar Abbas, Afsar Abbas, and Shukadev Mohanty, “A New signature of dark matter,” (1997), [arXiv:hep-ph/9709269](#).
- [49] “Nasa exoplanet catalog,” (2020).
- [50] A. Cassan, D. Kubas, J.-P. Beaulieu, M. Dominik, K. Horne, J. Greenhill, J. Wambsganss, J. Menzies, A. Williams, U. G. J  rgensen, and et al., “One or more bound planets per milky way star from microlensing observations,” *Nature* **481**, 167  169 (2012).
- [51] Basudeb Dasgupta, Ranjan Laha, and Anupam Ray, “Low Mass Black Holes from Dark Core Collapse,” (2020), [arXiv:2009.01825 \[astro-ph.HE\]](#).
- [52] R N Manchester, G B Hobbs, A Teoh, and M Hobbs, “The Australia Telescope National Facility pulsar catalogue,” *Astron. J.* **129**, 1993 (2005), [arXiv:astro-ph/0412641 \[astro-ph\]](#).
- [53] Max Camenzind, *Compact Objects in Astrophysics: White Dwarfs, Neutron Stars and Black Holes* (2007).
- [54] Dan Hooper and Jason H. Steffen, “Dark Matter And The Habitability of Planets,” *JCAP* **07**, 046 (2012), [arXiv:1103.5086 \[astro-ph.EP\]](#).
- [55] Jose A. Caballero, “A review on substellar objects beyond the deuterium burning mass limit: planets, brown dwarfs or what?” (2018), [arXiv:1808.07798 \[astro-ph.SR\]](#).
- [56] Andrew Gould *et al.* (MICROFUN, OGLE, ROBOTNET), “Microlens ogle-2005-blg-169 implies cool neptune-like planets are common,” *Astrophys. J. Lett.* **644**, L37–L40 (2006), [arXiv:astro-ph/0603276](#).
- [57] D. Saumon and Mark S. Marley, “The evolution of l and t dwarfs in color  magnitude diagrams,” *The Astrophysical Journal* **689**, 1327  1344 (2008).
- [58] S. K. Leggett, P. Tremblin, T. L. Esplin, K. L. Luhman, and Caroline V. Morley, “The y-type brown dwarfs: Estimates of mass and age from new astrometry, homogenized photometry, and near-infrared spectroscopy,” *The Astrophysical Journal* **842**, 118 (2017).
- [59] C. Reyl  l, P. Delorme, C. J. Willott, L. Albert, X. Delfosse, T. Forveille, E. Artigau, L. Malo, G. J. Hill, and R. Doyon, “The ultracool-field dwarf luminosity-function and space density from the canada-france brown dwarf survey,” *Astronomy & Astrophysics* **522**, A112 (2010).
- [60] Esther Buenzli, D  niel Apai, Caroline V. Morley, Davin Flateau, Adam P. Showman, Adam Burrows, Mark S. Marley, Nikole K. Lewis, and I. Neill Reid, “vertical atmospheric structure in a variable brown dwarf: pressure-dependent phase shifts in simultaneous hubble space telescope - spitzer light curves,” *The Astrophysical Journal* **760**, L31 (2012).
- [61] Beth A. Biller, Ian J. M. Crossfield, Luigi Mancini, Simona Ciceri, John Southworth, Taisiya G. Kopytova, Micka  l Bonnefoy, Niall R. Deacon, Joshua E. Schlieder, Esther Buenzli, and et al., “Weather on the nearest brown dwarfs: Resolved simultaneous multi-wavelength variability monitoring of wise j104915.57  531906.1ab,” *The Astrophysical Journal* **778**, L10 (2013).
- [62] Andrew R. Zentner and Andrew P. Hearin, “Asymmetric Dark Matter May Alter the Evolution of Low-mass Stars and Brown Dwarfs,” *Phys. Rev. D* **84**, 101302 (2011), [arXiv:1110.5919 \[astro-ph.CO\]](#).
- [63] Igor V. Moskalenko and Lawrence L. Wai, “Dark matter burners,” *The Astrophysical Journal* **659**, L29  L32 (2007).
- [64] Malcolm Fairbairn, Pat Scott, and Joakim Edsjo, “The Zero Age Main Sequence of WIMP burners,” *Phys. Rev. D* **77**, 047301 (2008), [arXiv:0710.3396 \[astro-ph\]](#).
- [65] Douglas Spolyar, Katherine Freese, and Paolo Gondolo, “Dark matter and the first stars: A new phase of stellar evolution,” *Physical Review Letters* **100** (2008), 10.1103/physrevlett.100.051101.
- [66] Katherine Freese, Peter Bodenheimer, Douglas Spolyar, and Paolo Gondolo, “Stellar structure of dark stars: A first phase of stellar evolution resulting from dark matter annihilation,” *The Astrophysical Journal* **685**, L101  L104 (2008).
- [67] Pat Scott, Malcolm Fairbairn, and Joakim Edsjo, “Dark stars at the Galactic centre - the main sequence,” *Mon. Not. Roy. Astron. Soc.* **394**, 82 (2009), [arXiv:0809.1871 \[astro-ph\]](#).
- [68] Marco Taoso, Gianfranco Bertone, Georges Meynet, and Silvia Ekstr  m, “Dark matter annihilations in population iii stars,” *Physical Review D* **78** (2008), 10.1103/physrevd.78.123510.
- [69] Katherine Freese, Paolo Gondolo, J.A. Sellwood, and Douglas Spolyar, “Dark Matter Densities during the Formation of the First Stars and in Dark Stars,” *Astrophys. J.* **693**, 1563–1569 (2009), [arXiv:0805.3540 \[astro-](#)

- ph].
- [70] Katherine Freese, Douglas Spolyar, and Anthony Aguirre, “Dark Matter Capture in the first star: a Power source and a limit on Stellar Mass,” *JCAP* **11**, 014 (2008), arXiv:0802.1724 [astro-ph].
- [71] Fabio Iocco, “Dark Matter Capture and Annihilation on the First Stars: Preliminary Estimates,” *Astrophys. J. Lett.* **677**, L1–L4 (2008), arXiv:0802.0941 [astro-ph].
- [72] Katherine Freese, Cosmin Ilie, Douglas Spolyar, Monica Valluri, and Peter Bodenheimer, “Supermassive dark stars: Detectable in jwst,” *The Astrophysical Journal* **716**, 1397a–1407 (2010).
- [73] Dan Hooper, Douglas Spolyar, Alberto Vallinotto, and Nickolay Y. Gnedin, “Inelastic Dark Matter As An Efficient Fuel For Compact Stars,” *Phys. Rev. D* **81**, 103531 (2010), arXiv:1002.0005 [hep-ph].
- [74] Jordi Casanellas and Ilídio Lopes, “Towards the use of asteroseismology to investigate the nature of dark matter,” *Monthly Notices of the Royal Astronomical Society* **410**, 535a–540 (2010).
- [75] Erik Zackrisson, Pat Scott, Claes-Erik Rydberg, Fabio Iocco, Bengt Edvardsson, GÅúran ÅÚstlin, Sofia Sivertsson, Adi Zitrin, Tom Broadhurst, and Paolo Gondolo, “Finding high-redshift dark stars with the james webb space telescope,” *The Astrophysical Journal* **717**, 257a–267 (2010).
- [76] Fabio Iocco, Marco Taoso, Florent Leclercq, and Georges Meynet, “Main sequence stars with asymmetric dark matter,” *Phys. Rev. Lett.* **108**, 061301 (2012), arXiv:1201.5387 [astro-ph.SR].
- [77] Cosmin Ilie, Katherine Freese, Monica Valluri, Ilian T. Iliev, and Paul R. Shapiro, “Observing supermassive dark stars with james webb space telescope,” *Monthly Notices of the Royal Astronomical Society* **422**, 2164a–2186 (2012).
- [78] Ilídio Lopes and Joseph Silk, “A particle dark matter footprint on the first generation of stars,” *Astrophys. J.* **786**, 25 (2014), arXiv:1404.3909 [astro-ph.CO].
- [79] José Lopes, Ilídio Lopes, and Joseph Silk, “Asteroseismology of red clump stars as a probe of the dark matter content of the galaxy central region,” *The Astrophysical Journal* **880**, L25 (2019).
- [80] Ebrahim Hassani, Reza Pazhouhesh, and Hossein Ebadi, “The effect of dark matter on stars at the galactic center: The paradox of youth problem,” *International Journal of Modern Physics D* **29**, 2050052 (2020).
- [81] Przemek MrÅsz, Andrzej Udalski, Jan Skowron, Radosław Poleski, Szymon Kozłowski, Michał K. Szymański, Igor Soszyński, Łukasz Wyrzykowski, Paweł Pietrukowicz, Krzysztof Ulaczyk, and et al., “No large population of unbound or wide-orbit jupiter-mass planets,” *Nature* **548**, 183a–186 (2017).
- [82] A. van Elteren, S. Portegies Zwart, I. Pelupessy, M. X. Cai, and S. L. W. McMillan, “Survivability of planetary systems in young and dense star clusters,” *Astronomy & Astrophysics* **624**, A120 (2019).
- [83] Michael Perryman, Joel Hartman, GÅaspÅr ÅA. Bakos, and Lennart Lindgren, “Astrometric exoplanet detection withgaia,” *The Astrophysical Journal* **797**, 14 (2014).
- [84] G. Fritz Benedict, Barbara E. McArthur, George Gatewood, Edmund Nelan, William D. Cochran, Artie Hatzes, Michael Endl, Robert Wittenmyer, Sallie L. Baliunas, Gordon A. H. Walker, and et al., “The extrasolar planet Ît eridani b: Orbit and mass,” *The Astronomical Journal* **132**, 2206a–2218 (2006).
- [85] Fabo Feng, Mikko Tuomi, and Hugh R. A. Jones, “Detection of the closest jovian exoplanet in the epsilon indi triple system,” (2018), arXiv:1803.08163 [astro-ph.EP].
- [86] Jeremy Bailey, R. Paul Butler, C. G. Tinney, Hugh R. A. Jones, Simon O’Toole, Brad D. Carter, and Geoffrey W. Marcy, “A jupiter-like planet orbiting the nearby m dwarf gj 832,” *The Astrophysical Journal* **690**, 743a–747 (2008).
- [87] R. Paul Butler, John Asher Johnson, Geoffrey W. Marcy, Jason T. Wright, Steven S. Vogt, and Debra A. Fischer, “A long-period jupiter-mass planet orbiting the nearby m dwarf gj 8491,” *Publications of the Astronomical Society of the Pacific* **118**, 1685a–1689 (2006).
- [88] A. P. Hatzes, W. D. Cochran, M. Endl, E. W. Guenther, S. H. Saar, G. A. H. Walker, S. Yang, M. Hartmann, M. Esposito, D. B. Paulson, and et al., “Confirmation of the planet hypothesis for the long-period radial velocity variations of Îsgeminorum,” *Astronomy & Astrophysics* **457**, 335a–341 (2006).
- [89] Geoffrey W. Marcy, R. Paul Butler, Debra A. Fischer, Greg Laughlin, Steven S. Vogt, Gregory W. Henry, and Dimitri Pourbaix, “A planet at 5 au around 55 cancri,” *The Astrophysical Journal* **581**, 1375a–1388 (2002).
- [90] M. Mayor, S. Udry, D. Naef, F. Pepe, D. Queloz, N. C. Santos, and M. Burnet, “The coralie survey for southern extra-solar planets,” *Astronomy & Astrophysics* **415**, 391a–402 (2004).
- [91] Artie P. Hatzes, William D. Cochran, Michael Endl, Barbara McArthur, Diane B. Paulson, Gordon A. H. Walker, Bruce Campbell, and Stephenson Yang, “A planetary companion to Îs cephei a,” *The Astrophysical Journal* **599**, 1383a–1394 (2003).
- [92] R. Paul Butler, Geoffrey W. Marcy, Debra A. Fischer, Timothy M. Brown, Adam R. Contos, Sylvain G. Korzennik, Peter Nisenson, and Robert W. Noyes, “Evidence for multiple companions to Î andromedae,” *The Astrophysical Journal* **526**, 916–927 (1999).
- [93] Philip C. Gregory and Debra A. Fischer, “A bayesian periodogram finds evidence for three planets in 47 Åcur-sae Åmajoris,” *Monthly Notices of the Royal Astronomical Society* **403**, 731a–747 (2010).
- [94] D. Naef, M. Mayor, S. G. Korzennik, D. Queloz, S. Udry, P. Nisenson, R. W. Noyes, T. M. Brown, J. L. Beuzit, C. Perrier, and et al., “The elodie survey for northern extra-solar planets,” *Astronomy & Astrophysics* **410**, 1051a–1054 (2003).
- [95] John Asher Johnson, R. Paul Butler, Geoffrey W. Marcy, Debra A. Fischer, Steven S. Vogt, Jason T. Wright, and Kathryn M. G. Peek, “A new planet around an m dwarf: Revealing a correlation between exoplanets and stellar mass,” *The Astrophysical Journal* **670**, 833a–840 (2007).
- [96] Debra Fischer, Peter Driscoll, Howard Isaacson, Matt Giguere, Geoffrey W. Marcy, Jeff Valenti, Jason T. Wright, Gregory W. Henry, John Asher Johnson, Andrew Howard, and et al., “Five planets and an independent confirmation of hd 196885ab from lick observatory,” *The Astrophysical Journal* **703**, 1545a–1556 (2009).
- [97] R. Luque, T. Trifonov, S. Reffert, A. Quirrenbach, M. H.

- Lee, S. Albrecht, M. Fredslund Andersen, V. Antoci, F. Grundahl, C. Schwab, and et al., “Precise radial velocities of giant stars,” *Astronomy & Astrophysics* **631**, A136 (2019).
- [98] Michael Endl, Erik J. Brugamyer, William D. Cochran, Phillip J. MacQueen, Paul Robertson, Stefano Meschiari, Ivan Ramirez, Matthew Shetrone, Kevin Gullikson, Marshall C. Johnson, and et al., “Two new long-period giant planets from the mcdonald observatory planet search and two stars with long-period radial velocity signals related to stellar activity cycles,” *The Astrophysical Journal* **818**, 34 (2016).
- [99] Brad D. Carter, R. Paul Butler, C. G. Tinney, Hugh R. A. Jones, Geoffrey W. Marcy, Chris McCarthy, Debra A. Fischer, and Alan J. Penny, “A planet in a circular orbit with a 6 year period,” *The Astrophysical Journal* **593**, L43â&#x2013;L46 (2003).
- [100] J. Rey, G. HÅ&#x211;brard, F. Bouchy, V. Bourrier, I. Boisse, N. C. Santos, L. Arnold, N. Astudillo-Defru, X. Bonfils, S. Borgniet, and et al., “The sophie search for northern extrasolar planets,” *Astronomy & Astrophysics* **601**, A9 (2017).
- [101] Geoffrey W. Marcy, R. Paul Butler, Steven S. Vogt, Debra A. Fischer, Gregory W. Henry, Greg Laughlin, Jason T. Wright, and John A. Johnson, “Five new extrasolar planets,” *The Astrophysical Journal* **619**, 570–584 (2005).
- [102] Steven S. Vogt, R. Paul Butler, Geoffrey W. Marcy, Debra A. Fischer, Dimitri Pourbaix, Kevin Apps, and Gregory Laughlin, “Ten lowâ&#x2013;mass companions from the keck precision velocity survey,” *The Astrophysical Journal* **568**, 352â&#x2013;362 (2002).
- [103] Samuel W. Yee, Erik A. Petigura, Benjamin J. Fulton, Heather A. Knutson, Konstantin Batygin, GÅ&#x211;aspÅ&#x211;ar Å&#x211;A. Bakos, Joel D. Hartman, Lea A. Hirsch, Andrew W. Howard, Howard Isaacson, and et al., “Harp-11: Discovery of a second planet and a clue to understanding exoplanet obliquities,” *The Astronomical Journal* **155**, 255 (2018).
- [104] J. T. Wright, S. Upadhyay, G. W. Marcy, D. A. Fischer, Eric B. Ford, and John Asher Johnson, “Ten new and updated multiplanet systems and a survey of exoplanetary systems,” *The Astrophysical Journal* **693**, 1084â&#x2013;1099 (2009).
- [105] A. Niedzielski, G. Nowak, M. AdamÅ&#x211;sw, and A. Wolsczan, “Substellar-mass companions to the k-dwarf bd+14 4559 and the k-giants hd 240210 and bd+20 2457,” *The Astrophysical Journal* **707**, 768â&#x2013;777 (2009).
- [106] M. Marmier, D. SÅ&#x211;gransan, S. Udry, M. Mayor, F. Pepe, D. Queloz, C. Lovis, D. Naef, N. C. Santos, R. Alonso, and et al., “The coralie survey for southern extrasolar planets,” *Astronomy & Astrophysics* **551**, A90 (2013).
- [107] D. Naef, M. Mayor, G. Lo Curto, F. Bouchy, C. Lovis, C. Moutou, W. Benz, F. Pepe, D. Queloz, N. C. Santos, and et al., “The harps search for southern extrasolar planets,” *Astronomy & Astrophysics* **523**, A15 (2010).
- [108] R. Paul Butler, Geoffrey W. Marcy, Steven S. Vogt, Debra A. Fischer, Gregory W. Henry, Gregory Laughlin, and Jason T. Wright, “Seven new keck planets orbiting g and k dwarfs,” *The Astrophysical Journal* **582**, 455–466 (2003).
- [109] BunÅ&#x211;zei Sato, Masashi Omiya, Robert A. Wittenmyer, Hiroki Harakawa, Makiko Nagasawa, Hideyuki Izumiura, Eiji Kambe, Yoichi Takeda, Michitoshi Yoshida, Yoichi Itoh, and et al., “A double planetary system around the evolved intermediate-mass star hd 4732,” *The Astrophysical Journal* **762**, 9 (2012).
- [110] Robert A. Wittenmyer, Jonathan Horner, C. G. Tinney, R. P. Butler, H. R. A. Jones, Mikko Tuomi, G. S. Salter, B. D. Carter, F. Elliott Koch, S. J. OÅ&#x211;Toole, and et al., “The anglo-australian planet search. xxiii. two new jupiter analogs,” *The Astrophysical Journal* **783**, 103 (2014).
- [111] Jeff A. Valenti, Debra Fischer, Geoffrey W. Marcy, John A. Johnson, Gregory W. Henry, Jason T. Wright, Andrew W. Howard, Matt Giguere, and Howard Isaacson, “Two exoplanets discovered at keck observatory,” *The Astrophysical Journal* **702**, 989â&#x2013;997 (2009).
- [112] L. Mancini, J. Lillo-Box, J. Southworth, L. Borsato, D. Gandolfi, S. Ciceri, D. Barrado, R. Brahm, and Th. Henning, “Kepler-539: A young extrasolar system with two giant planets on wide orbits and in gravitational interaction,” *Astronomy & Astrophysics* **590**, A112 (2016).
- [113] Kailash C. Sahu, Stefano Casertano, Howard E. Bond, Jeff Valenti, T. Ed Smith, Dante Minniti, Manuela Zoccali, Mario Livio, Nino Panagia, Nikolai Piskunov, and et al., “Transiting extrasolar planetary candidates in the galactic bulge,” *Nature* **443**, 534â&#x2013;540 (2006).
- [114] Etienne Bachelet and Matthew Penny, “WFIRST and EUCLID: Enabling the microlensing parallax measurement from space,” *The Astrophysical Journal* **880**, L32 (2019).
- [115] Przemek MrÅ&#x211;sz, RadosÅ&#x211;aw Poleski, Cheongho Han, Andrzej Udalski, Andrew Gould, MichaÅ&#x211; K. SzymaÅ&#x211;ski, Igor SoszyÅ&#x211;ski, PaweÅ&#x211; Pietrukowicz, Szymon KozÅ&#x211;owski, Jan Skowron, and et al., “A free-floating or wide-orbit planet in the microlensing event ogle-2019-blg-0551,” *The Astronomical Journal* **159**, 262 (2020).
- [116] Wei Zhu *et al.*, “mass measurements of isolated objects from space-based microlensing,” *The Astrophysical Journal* **825**, 60 (2016).
- [117] Yossi Shvartzvald *et al.*, “Spitzer microlensing parallax for OGLE-2017-BLG-0896 reveals a counter-rotating low-mass brown dwarf,” *The Astronomical Journal* **157**, 106 (2019).
- [118] J. Green *et al.*, “Wide-field infrared survey telescope (wfirst) final report,” (2012), [arXiv:1208.4012 \[astro-ph.IM\]](https://arxiv.org/abs/1208.4012).
- [119] Samson A. Johnson, Matthew Penny, B. Scott Gaudi, Eamonn Kerins, Nicholas J. Rattenbury, Annie C. Robin, Sebastiano Calchi Novati, and Calen B. Henderson, “Predictions of the nancy grace roman space telescope galactic exoplanet survey. II. free-floating planet detection rates,” *The Astronomical Journal* **160**, 123 (2020).
- [120] John Stauffer, George Helou, Robert A. Benjamin, Massimo Marengo, J. Davy Kirkpatrick, Peter Capak, Mansi Kasliwal, James M. Bauer, Dante Minniti, John Bally, Nicolas Lodieu, Brendan Bowler, ZengHua Zhang, Sean J. Carey, Stefanie Milam, and Bryan Holler, “The science advantage of a redder filter for wfirst,” (2018), [arXiv:1806.00554 \[astro-ph.GA\]](https://arxiv.org/abs/1806.00554).



- [121] Doris Breuer Tilman Spohn and Torrence V. Johnson, “Encyclopedia of the solar system,” **5** (2014), [10.1016/C2010-0-67309-3](#).
- [122] Sayantan Auddy, Shantanu Basu, and S. R. Valluri, “Analytic models of brown dwarfs and the substellar mass limit,” *Advances in Astronomy* **2016**, 1715 (2016).
- [123] Julio F. Navarro, Carlos S. Frenk, and Simon D. M. White, “The structure of cold dark matter halos,” *The Astrophysical Journal* **462**, 563 (1996).
- [124] Oleg Y. Gnedin, Daniel Ceverino, Nickolay Y. Gnedin, Anatoly A. Klypin, Andrey V. Kravtsov, Robyn Levine, Daisuke Nagai, and Gustavo Yepes, “Halo contraction effect in hydrodynamic simulations of galaxy formation,” (2011), [arXiv:1108.5736 \[astro-ph.CO\]](#).
- [125] A. Burkert, “The structure of dark matter halos in dwarf galaxies,” *The Astrophysical Journal* **447** (1995), [10.1086/309560](#).
- [126] Timothy Cohen, Mariangela Lisanti, Aaron Pierce, and Tracy R. Slatyer, “Wino Dark Matter Under Siege,” *JCAP* **10**, 061 (2013), [arXiv:1307.4082 \[hep-ph\]](#).
- [127] Miguel Pato, Fabio Iocco, and Gianfranco Bertone, “Dynamical constraints on the dark matter distribution in the milky way,” *Journal of Cosmology and Astroparticle Physics* **2015**, 001â€š001 (2015).
- [128] Raghuvver Garani and Sergio Palomares-Ruiz, “Dark matter in the Sun: scattering off electrons vs nucleons,” *JCAP* **05**, 007 (2017), [arXiv:1702.02768 \[hep-ph\]](#).
- [129] A. Sommerfeld, “Über die beugung und bremsung der elektronen,” *Annalen der Physik* **403**, 257 (1931).
- [130] Hai-Nan Lin and Xin Li, “The Dark Matter Profiles in the Milky Way,” *Mon. Not. Roy. Astron. Soc.* **487**, 5679–5684 (2019), [arXiv:1906.08419 \[astro-ph.GA\]](#).
- [131] Jonathan Brande, Thomas Barclay, Joshua E. Schlieder, Eric D. Lopez, and Elisa V. Quintana, “The feasibility of directly imaging nearby cold jovian planets with miri/jwst,” *The Astronomical Journal* **159**, 18 (2019).
- [132] Jurg Diemand, Michael Kuhlen, and Piero Madau, “Dark matter substructure and gamma-ray annihilation in the milky way halo,” *The Astrophysical Journal* **657**, 262â€š270 (2007).
- [133] J. Diemand, M. Kuhlen, P. Madau, M. Zemp, B. Moore, D. Potter, and J. Stadel, “Clumps and streams in the local dark matter distribution,” *Nature* **454**, 735â€š738 (2008).
- [134] J. Stadel, D. Potter, B. Moore, J. Diemand, P. Madau, M. Zemp, M. Kuhlen, and V. Quilis, “Quantifying the heart of darkness with ghalo - a multibillion particle simulation of a galactic halo,” *Monthly Notices of the Royal Astronomical Society: Letters* **398**, L21â€šL25 (2009).
- [135] V. Springel, J. Wang, M. Vogelsberger, A. Ludlow, A. Jenkins, A. Helmi, J. F. Navarro, C. S. Frenk, and S. D. M. White, “The aquarius project: the subhaloes of galactic haloes,” *Monthly Notices of the Royal Astronomical Society* **391**, 1685â€š1711 (2008).
- [136] R. Benton Metcalf and Piero Madau, “Compound gravitational lensing as a probe of dark matter substructure within galaxy halos,” *Astrophys. J.* **563**, 9 (2001), [arXiv:astro-ph/0108224](#).
- [137] M. dal Ponte et al., “Increasing the census of L and T dwarfs in wide binary and multiple systems using Dark Energy Survey DR1 and Gaia DR2 data,” [arXiv:2001.11015 \[astro-ph\]](#).
- [138] E. Valenti, M. Zoccali, O. A. Gonzalez, D. Minniti, J. Alonso-García, E. Marchetti, M. Hempel, A. Renzini, and M. Rejkuba, “Stellar density profile and mass of the milky way bulge from vvv data,” *Astronomy & Astrophysics* **587**, L6 (2016).
- [139] Emmanuel Moulin (H.E.S.S.), “The inner 300 parsecs of the Milky Way seen by H.E.S.S.: a Pevatron in the Galactic Centre,” *EPJ Web Conf.* **136**, 03017 (2017).
- [140] C. M. Dutra, B. X. Santiago, E. L. D. Bica, and B. Barbuy, “Extinction within 10 kpc of the Galactic centre using 2MASS,” *Monthly Notices of the Royal Astronomical Society* **338**, 253–262 (2003).
- [141] C. M. Dutra, B. X. Santiago, and E. Bica, “Low-extinction windows in the inner galactic bulge,” *Astronomy & Astrophysics* **381**, 219â€š226 (2002).
- [142] Matthew C. Digman, Christopher V. Cappiello, John F. Beacom, Christopher M. Hirata, and Annika H.G. Peter, “Not as big as a barn: Upper bounds on dark matter-nucleus cross sections,” *Phys. Rev. D* **100**, 063013 (2019), [arXiv:1907.10618 \[hep-ph\]](#).
- [143] Joseph Bramante, Antonio Delgado, and Adam Martin, “Multiscatter stellar capture of dark matter,” *Phys. Rev. D* **96**, 063002 (2017), [arXiv:1703.04043 \[hep-ph\]](#).
- [144] Cosmin Ilie, Jacob Pilawa, and Saiyang Zhang, “Comment on ‘Multiscatter stellar capture of dark matter’,” *Phys. Rev. D* **102**, 048301 (2020), [arXiv:2005.05946 \[astro-ph.CO\]](#).
- [145] Tristan Guillot and Daniel Gautier, “Giant Planets,” (2009) [arXiv:0912.2019 \[astro-ph.EP\]](#).
- [146] L. Vocollo J. Brodholt D. Alfe, M. J. Gillan and G. D. Price, “The ab initio simulation of the Earth’s core,” *Royal Society* **360**, 1795 (2002).
- [147] K. Griest and D. Seckel, “Cosmic Asymmetry, Neutrinos and the Sun,” *Nucl. Phys. B* **283**, 681–705 (1987), [Erratum: *Nucl.Phys.B* 296, 1034–1036 (1988)].
- [148] Yonit Hochberg, Eric Kuflik, Tomer Volansky, and Jay G. Wacker, “Mechanism for Thermal Relic Dark Matter of Strongly Interacting Massive Particles,” *Phys. Rev. Lett.* **113**, 171301 (2014), [arXiv:1402.5143 \[hep-ph\]](#).
- [149] Nicola Andrea Dondi, Francesco Sannino, and Juri Smirnov, “Thermal history of composite dark matter,” *Phys. Rev. D* **101**, 103010 (2020), [arXiv:1905.08810 \[hep-ph\]](#).
- [150] R. Agnese et al. (SuperCDMS), “Low-mass dark matter search with CDMSlite,” *Phys. Rev. D* **97**, 022002 (2018), [arXiv:1707.01632 \[astro-ph.CO\]](#).
- [151] J.I. Collar, “Search for a nonrelativistic component in the spectrum of cosmic rays at Earth,” *Phys. Rev. D* **98**, 023005 (2018), [arXiv:1805.02646 \[astro-ph.CO\]](#).
- [152] A.H. Abdelhameed et al. (CRESST), “First results from the CRESST-III low-mass dark matter program,” *Phys. Rev. D* **100**, 102002 (2019), [arXiv:1904.00498 \[astro-ph.CO\]](#).
- [153] Dan Hooper and Samuel D. McDermott, “Robust Constraints and Novel Gamma-Ray Signatures of Dark Matter That Interacts Strongly With Nucleons,” *Phys. Rev. D* **97**, 115006 (2018), [arXiv:1802.03025 \[hep-ph\]](#).
- [154] Torsten Bringmann and Maxim Pospelov, “Novel direct detection constraints on light dark matter,” *Phys. Rev. Lett.* **122**, 171801 (2019), [arXiv:1810.10543 \[hep-ph\]](#).
- [155] Juri Smirnov and John F. Beacom, “Co-SIMP Miracle,” (2020), [arXiv:2002.04038 \[hep-ph\]](#).



- [156] P. Di Gangi (XENON), “Results of the 1 tonne D7 year WIMP search with XENON1T,” *Nuovo Cim. C* **42**, 76 (2019).
- [157] E. Aprile *et al.* (XENON), “Constraining the spin-dependent WIMP-nucleon cross sections with XENON1T,” *Phys. Rev. Lett.* **122**, 141301 (2019), [arXiv:1902.03234 \[astro-ph.CO\]](#).
- [158] Christopher V. Capiello, Kenny C. Y. Ng, and John F. Beacom, “Reverse Direct Detection: Cosmic Ray Scattering With Light Dark Matter,” *Phys. Rev. D* **99**, 063004 (2019), [arXiv:1810.07705 \[hep-ph\]](#).
- [159] Yohei Ema, Filippo Sala, and Ryosuke Sato, “Light Dark Matter at Neutrino Experiments,” *Phys. Rev. Lett.* **122**, 181802 (2019), [arXiv:1811.00520 \[hep-ph\]](#).
- [160] Christopher Capiello and John F. Beacom, “Strong New Limits on Light Dark Matter from Neutrino Experiments,” *Phys. Rev. D* **100**, 103011 (2019), [arXiv:1906.11283 \[hep-ph\]](#).
- [161] Rouven Essig, Aaron Manalaysay, Jeremy Mardon, Peter Sorensen, and Tomer Volansky, “First direct detection limits on sub-gev dark matter from xenon10,” *Physical Review Letters* **109** (2012), [10.1103/physrevlett.109.021301](#).
- [162] Rouven Essig, Tomer Volansky, and Tien-Tien Yu, “New constraints and prospects for sub-gev dark matter scattering off electrons in xenon,” *Physical Review D* **96** (2017), [10.1103/physrevd.96.043017](#).
- [163] J. Angle, E. Aprile, F. Arneodo, L. Baudis, A. Bernstein, A. I. Bolozdynya, L. C. C. Coelho, C. E. Dahl, L. De Viveiros, A. D. Ferella, and et al., “Search for light dark matter in xenon10 data,” *Physical Review Letters* **107** (2011), [10.1103/physrevlett.107.051301](#).
- [164] E. Aprile, J. Aalbers, F. Agostini, M. Alfonsi, F. ÅLD. Amaro, M. Anthony, F. Arneodo, P. Barrow, L. Baudis, B. Bauermeister, and et al., “Low-mass dark matter search using ionization signals in xenon100,” *Physical Review D* **94** (2016), [10.1103/physrevd.94.092001](#).
- [165] P. Agnes, I. ÅLF. ÅLM. Albuquerque, T. Alexander, A. ÅLK. Alton, G. ÅLR. Araujo, D. ÅLM. Asner, M. Ave, H. ÅEO. Back, B. Baldin, G. Batignani, and et al., “Constraints on sub-gev dark-matterâŠelectron scattering from the darkside-50 experiment,” *Physical Review Letters* **121** (2018), [10.1103/physrevlett.121.111303](#).
- [166] R. Agnese, T. Aralis, T. Aramaki, I. ÅLJ. Arnquist, E. Azadbakht, W. Baker, S. Banik, D. Barker, D. ÅLA. Bauer, T. Binder, and et al., “First dark matter constraints from a supercdms single-charge sensitive detector,” *Physical Review Letters* **121** (2018), [10.1103/physrevlett.121.051301](#).
- [167] Michael Crisler, Rouven Essig, Juan Estrada, Guillermo Fernandez, Javier Tiffenberg, Miguel Sofo Haro, Tomer Volansky, and Tien-Tien Yu, “Sensei: First direct-detection constraints on sub-gev dark matter from a surface run,” *Physical Review Letters* **121** (2018), [10.1103/physrevlett.121.061803](#).
- [168] Orr Abramoff, Liron Barak, Itay M. Bloch, Luke Chaplinsky, Michael Crisler, Dawa, Alex Drlica-Wagner, Rouven Essig, Juan Estrada, Erez Etzion, and et al., “Sensei: Direct-detection constraints on sub-gev dark matter from a shallow underground run using a prototype skipper ccd,” *Physical Review Letters* **122** (2019), [10.1103/physrevlett.122.161801](#).
- [169] A. Aguilar-Arevalo, D. Amidei, D. Baxter, G. Canceledo, B. ÅLA. Cervantes Vergara, A. ÅLE. Chavarria, E. Darragh-Ford, J. ÅLR. ÅLT. de Mello Neto, J. ÅLC. D. ÅZOlivo, J. Estrada, and et al., “Constraints on light dark matter particles interacting with electrons from damic at snolab,” *Physical Review Letters* **123** (2019), [10.1103/physrevlett.123.181802](#).
- [170] Liron Barak *et al.*, “Sensei: Direct-detection results on sub-gev dark matter from a new skipper-ccd,” (2020), [arXiv:2004.11378 \[astro-ph.CO\]](#).
- [171] EDELWEISS Collaboration, “First germanium-based constraints on sub-mev dark matter with the edelweiss experiment,” (2020), [arXiv:2003.01046 \[astro-ph.GA\]](#).
- [172] D.W. Amaral *et al.* (SuperCDMS), “Constraints on low-mass, relic dark matter candidates from a surface-operated SuperCDMS single-charge sensitive detector,” (2020), [arXiv:2005.14067 \[hep-ex\]](#).
- [173] Haipeng An, Maxim Pospelov, Josef Pradler, and Adam Ritz, “Directly Detecting MeV-scale Dark Matter via Solar Reflection,” *Phys. Rev. Lett.* **120**, 141801 (2018), [Erratum: *Phys.Rev.Lett.* 121, 259903 (2018)], [arXiv:1708.03642 \[hep-ph\]](#).
- [174] Timon Emken, Chris Kouvaris, and Niklas Gr. Åynlund Nielsen, “The sun as a sub-gev dark matter accelerator,” *Physical Review D* **97** (2018), [10.1103/physrevd.97.063007](#).
- [175] Patrick J. Fox and Erich Poppitz, “Leptophilic Dark Matter,” *Phys. Rev. D* **79**, 083528 (2009), [arXiv:0811.0399 \[hep-ph\]](#).
- [176] Joachim Kopp, Viviana Niro, Thomas Schwetz, and Jure Zupan, “DAMA/LIBRA and leptonically interacting Dark Matter,” *Phys. Rev. D* **80**, 083502 (2009), [arXiv:0907.3159 \[hep-ph\]](#).
- [177] Joachim Kopp, Lisa Michaels, and Juri Smirnov, “Loopy Constraints on Leptophilic Dark Matter and Internal Bremsstrahlung,” *JCAP* **04**, 022 (2014), [arXiv:1401.6457 \[hep-ph\]](#).
- [178] Nicole F. Bell, Yi Cai, Rebecca K. Leane, and Anibal D. Medina, “Leptophilic dark matter with  $Z$  interactions,” *Phys. Rev. D* **90**, 035027 (2014), [arXiv:1407.3001 \[hep-ph\]](#).
- [179] Francesco D’Eramo, Bradley J. Kavanagh, and Paolo Panci, “Probing Leptophilic Dark Sectors with Hadronic Processes,” *Phys. Lett. B* **771**, 339–348 (2017), [arXiv:1702.00016 \[hep-ph\]](#).
- [180] Glenn D. Starkman, Andrew Gould, Rahim Esmailzadeh, and Savas Dimopoulos, “Opening the Window on Strongly Interacting Dark Matter,” *Phys. Rev. D* **41**, 3594 (1990).
- [181] Felix Kahlhoefer, Kai Schmidt-Hoberg, Thomas Schwetz, and Stefan Vogl, “Implications of unitarity and gauge invariance for simplified dark matter models,” *JHEP* **02**, 016 (2016), [arXiv:1510.02110 \[hep-ph\]](#).
- [182] Nicole F. Bell, Yi Cai, and Rebecca K. Leane, “Dark Forces in the Sky: Signals from  $Z'$  and the Dark Higgs,” *JCAP* **08**, 001 (2016), [arXiv:1605.09382 \[hep-ph\]](#).
- [183] Nicole F. Bell, Yi Cai, and Rebecca K. Leane, “Impact of mass generation for spin-1 mediator simplified models,” *JCAP* **01**, 039 (2017), [arXiv:1610.03063 \[hep-ph\]](#).
- [184] Michael Duerr, Felix Kahlhoefer, Kai Schmidt-Hoberg, Thomas Schwetz, and Stefan Vogl, “How to save the WIMP: global analysis of a dark matter model with two s-channel mediators,” *JHEP* **09**, 042 (2016),

- [arXiv:1606.07609 \[hep-ph\]](#).
- [185] Nicole F. Bell, Yi Cai, James B. Dent, Rebecca K. Leane, and Thomas J. Weiler, “Enhancing Dark Matter Annihilation Rates with Dark Bremsstrahlung,” *Phys. Rev. D* **96**, 023011 (2017), [arXiv:1705.01105 \[hep-ph\]](#).
- [186] Yanou Cui and Francesco D’Eramo, “Surprises from complete vector portal theories: New insights into the dark sector and its interplay with Higgs physics,” *Phys. Rev. D* **96**, 095006 (2017), [arXiv:1705.03897 \[hep-ph\]](#).
- [187] Simon Knapen, Tongyan Lin, and Kathryn M. Zurek, “Light Dark Matter: Models and Constraints,” *Phys. Rev. D* **96**, 115021 (2017), [arXiv:1709.07882 \[hep-ph\]](#).